國立臺灣大學工學院土木工程學系

碩士論文

Department of Civil Engineering

College of Engineering

National Taiwan University

Master Thesis

通過車輛偵測器資料分析與視覺化探索壅塞擴散模式

Exploring the Propagation Pattern of Traffic Congestion
Through Analyzing and Visualizing Vehicle Detector Data

許家維

Chia-Wei Hsu

指導教授：許聿廷 博士

Advisor: Yu-Ting Hsu, Ph.D.

中華民國 107 年 7 月

July, 2018

國立臺灣大學碩士學位論文
口試委員會審定書

通過車輛偵測器資料分析與視覺化探索壅塞擴散模式
Exploring the Propagation Pattern of Traffic Congestion
Through Analyzing and Visualizing Vehicle Detector Data

本論文係許家維君（R05521510）在國立臺灣大學土木工程學系
完成之碩士學位論文，於民國 107 年 7 月 17 日承下列考試委員審查通
過及口試及格，特此證明

口試委員：

_____（簽名）

（指導教授）

陳 柏 華　　　　_____

郭 佩 棻　　　　_____

系主任、所長　_____（簽名）

誌謝

其實有點難以置信，論文寫作終於也進入了尾聲，我想我會懷念這段安靜而專注的日子。人生有許多事情，正如船後的波紋，總要過後才覺得美，我想念交通組就是其中之一。大三升大四的暑假鼓起勇氣敲開了小許老師辦公室的門、面試時大許老師讓我當場做一首詩、修課做研究時咒罵著跑不出結果的 code、無數個夜晚的挑燈夜戰、論文寫作的過程與口試，種種情景都還歷歷在目。過程當中，雖然有過徬徨，有過迷惘；想過逃避，也想過放棄，更曾經懷疑過自己到底在幹嘛，但只要想起愛因斯坦說過的話，低潮與失落也就煙消雲散，如果我們知道我們在做什麼，那麼這就不叫研究了，不是嗎？儘管在這研究中，仍有許多力有未逮之處，但我仍然慶幸自己堅持到了最後一刻。也許多年後，我會忘記寫過的論文細節，但曾經幫助過我的人、始終支持著我的人，我將會一直銘記在心。

轉眼間在台大待了整整六年，我衷心的感謝這一路上所遇到的師長，讓對學術的嚴謹、批判的思辨與人文關懷內化到我的生命中，形塑成一種人生的哲學與處世的態度。尤其是領我進門並指導論文的許聿廷老師，不僅在理論知識上不厭其煩地教導，也願意給予學生的研究探索空間、啟發與支持，讓我看見一位好老師的榜樣。感謝 Albert 老師、朱致遠老師、賴勇成老師、大許老師在課堂當中的鼓勵、指教甚至是當頭棒喝，讓我懂得謙卑、懂得踏實，也依舊懂得作夢。感謝 Adrian 與 Way 老師，引我進入英文寫作的領域，並提供無數寶貴意見，使論文更臻完善。

在探討壅塞的研究過程當中，自己也常常卡在泥淖中，停滯不前、找不到出口，好在有你們，讓一切困難都迎刃而解。感謝小許家的夥伴柏傑總是走在最前面，至佑總是在身邊，讓我在無助的時候有人引導、有人陪伴；乃慈、毓軒、思文、書廷、宜萱、香吟、文宇像哥哥姊姊般一直以來的照顧，即使外宿依然能感受到家的溫暖。謝謝士淵，願意和我聊彼此的心裡話，以及每周三再忙都要赴約的茶湯會；謝謝研究室的室友任宏、明華、子皓、韻如、柏維、郁方、子鈞、依穎、Umav、俊嘉、大包、婉菁、晟松、洵顏在課業上的互相幫忙、球場上的默契搭檔、精神上的勉勵以及實質上的餵食；謝謝學弟妹譽仁、明儀、薇旦、子鈺、智勛、冠頡、儒斌、浩雅、妤庭、祝銘，時常能夠有一些想法的交換，並提供我許多建議；謝謝水服的彥伯、仲皓、承勳、志浩、祝姐、星魚、信總、34 期夥伴、36 期小浩浩們，成全了我的碧海與藍天；感謝養育、支持我的爸媽，謝謝你們賜予我健康的身體與衣食無缺的成長環境，讓我能夠專心於學業而無後顧之憂；謝謝交控中心同仁提供研究所需的資料、瓅凱學長提供技術上的協助，才能有今天的成果。感謝兩位口試委員以及林育生技正所給予的鼓勵與寶貴建議，衷心盼望藉由這篇論文的淺薄見解，能拋磚引玉讓相關議題持續被更多人重視、討論與探究。

2018 年 8 月 6 日，鎮守在土木系館 3 樓的第 693 天。雖然不捨，但終究還是必須離開，邁向一段嶄新的旅程。期望自己別忘那一年，那一天，出發時心中的夢。莫忘初衷。

祝福所有關心我的朋友們平安快樂。

<div align="right">

許家維 謹誌

2018 年夏 於土 314

</div>

中文摘要

對於交通管理而言,道路交通狀況的監測是很重要的課題,而如何監控和避免道路壅塞是交通管理最主要關心的面向之一。壅塞發生的原因包括自用車使用率提升使得車流量增加、道路系統容量不足或設計不良,以及事故或施工導致車道容量縮減等。而壅塞的影響層面則包括通勤時間的增長、駕駛人情緒上的負面衝擊、生活品質的降低以及在緊急應變上的潛在威脅。因此,深入了解這些壅塞所影響的範圍與層面,並找出道路系統中可能的瓶頸處,提供可靠資訊予用路人與交通管理單位作為參考,將可協助對於預防壅塞更積極的作為,並在交通管理策略上做出改善。

過去文獻中,針對不同資料來源所進行的交通狀態與事件偵測、壅塞擴散模式與資料視覺化皆有相關研究與討論,本研究將基於高解析度之車輛偵測器資料分析,將資料處理、模式辨識與視覺化三個區塊一併納入,建立一個完整的壅塞分析架構。本研究首先進行原始車輛偵測器資料的清理,處理資料中缺失與錯誤的問題,並篩選出後續分析所需要的特定資料,並根據與不同的壅塞界定門檻值,定義出壅塞發生的時空位置。本研究以車輛偵測器的實際位置,地圖圖資與鄰接矩陣的觀念建立路網。接著使用調整的核密度推估方法進行壅塞擴散模式的分析,在不同時間段進行案例分析,探討一階、二階鄰接以及不同轉向的上游路段受下游壅塞源頭影響的情形,歸納出可供參考的壅塞擴散模式和推估原則,並透過視覺化呈現交通車流資料的變化特性。

藉由案例分析的不同情境設定,與不同尺度的視覺化結果,將可以從圖面上觀察到整體路網當中有較高機率發生壅塞的位置,以及各源頭路段發生壅塞之後,傳遞的方向與影響程度。在路網中大部分的路段上觀察到的現象符合一些一般性的原則,上游路段受到壅塞的影響,一階鄰接路段大於二階鄰接路段;另外在相同鄰接度的情形下,直行進入下游路段大於左轉進入下游路段,左轉進入下游路段又大於右轉進入下游路段。
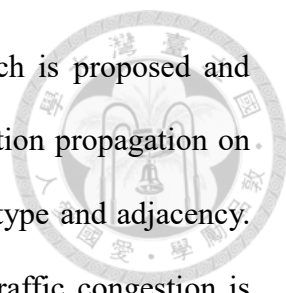
關鍵字: 車輛偵測器、核密度估計、交通狀態偵測、壅塞擴散模式、視覺化

ABSTRACT

The monitoring of roadway traffic conditions is critical for traffic management, where the detection of traffic congestion is one of major concerns. Traffic congestion may have various causes, including the increase of traffic volume due to higher private vehicle usage, inappropriate design or lack of capacity of road network and layout changes on the road segment owing to non-recurrent incidents such as traffic accidents or construction work. Traffic congestion may lead to the rise of commuting time, negative impact of driver physiology, lower quality of life and potential hazard on emergency response could be the impact of traffic congestion. Hence, further understanding of how traffic congestion was formed, propagated and dissipates, and identifying possible bottlenecks are critical for overall traffic management. Based on the relevant knowledge, it is possible to provide drivers and traffic management agencies reliable information to more actively prevent traffic congestion and thereby improve the quality of traffic management strategies.

In the current literature, traffic state detection, congestion propagation pattern and traffic data visualization have been studied and discussed, respectively. Based on high-resolution VD data, this study integrates the consideration of data processing, pattern recognition and visualization to develop a data analysis framework for better understanding of traffic congestion in an urban network. Data cleaning is first performed to deal with the missing and erroneous data, and then a specific data set needed for further analysis is extracted. Based on different thresholds of congestion detection, the spatio-temporal locations of congestion occurrences are recorded. The network structure is constructed based on the actual coordinate of VDs, map information and the concept of

the adjacent matrix. An adjusted kernel density estimation approach is proposed and applied to case studies, in order to investigate the effects of congestion propagation on road segments with different characteristics in terms of connection type and adjacency. Finally, a general principle describing the propagation pattern of traffic congestion is concluded and presented through data visualization.

Based on different scenarios for the case study and visualization result under different scales, locations with higher probability to be congested in the whole network and the propagation direction and impact after congestion occurred can be observed. Most of the road segments within the network follows some general principles. In terms of the impact on upstream road segments, road segments of the 1st order adjacency receive larger impact than road segments of the 2nd order adjacency. In addition, for road segments of the same order adjacency, which goes straight to the congested road segment is affected most by the source. The segment with a left turn comes second and the segment with a right turn receives the least influence.

CONTENTS

LIST OF FIGURES

LIST OF TABLES

Chapter 1   Introduction

1.1   Background

Traffic congestion is one of the main focuses of traffic management. It is a state when traffic demand exceeds roadway capacity. The characteristic of traffic congestion occurring within urban road networks can be quite different from those taking place on freeways because of traffic signals, intersections and the complexity of road networks. Traffic congestion can be further divided into recurrent one which usually occurs during peak hours and non-recurrent one resulting from a variety of incidents, such as traffic accidents, road construction as well as large activities.

Researchers are interested in several related topics, including the formation of traffic congestion, the estimation of negative effects caused by traffic congestion, the bottlenecks in the road network and the strategies to prevent as well as ease congestion. To answer the questions mentioned above, congestion incidents need to be identified from traffic data first. How to detect traffic congestion through a systematic approach of collecting and analyzing traffic data has been the key issue for traffic management. In previous studies, traffic data are often extracted from loop detectors. However, there are some obvious shortcomings, such as the difficulties in facility maintenance, high malfunctioning and misdetection rate. Hence, other types facilities for detection, for example, electronic toll collection (ETC) sensors, monitors and microwave vehicle detectors (VD) are installed. ETC system has been operating on the freeways in Taiwan since 2014. Besides improving the service level of the freeway system, it also contributes to the collection of large amount of traffic data. These data can be used for traffic

1

management and opened to both academia and individuals for extended applications. In Taipei City, vehicle detectors are widely installed within the urban road network, and high-resolution traffic data are collected. They provide abundant traffic data including point travel speed, traffic volume and occupancy. The daily VD data are provided without charge on the governmental open data platform, Data.Taipei website. Through the investigation of these data, the characteristics of traffic flows can be observed and a baseline traffic condition can be determined. By comparing the traffic data of a set of target VDs within a Region Of Interest (ROI) during a certain time interval with the baseline, congestion incidents can be detected. Traffic congestion may be manifested as a chain reaction, forming a shockwave across a certain scope of a roadway network (Li, She, Luo, & Yu, 2013). Some studies on traffic congestion forecasting have been conducted by employing pheromone communication models (Kurihara, Tamaki, Numao, Yano, Kagawa, & Morita, 2009), density wave models (Nagatani, 2002) and so on. To understand how a congestion incident may propagate throughout a network and dissipate based on the exploration of real data can be the research direction to further enhance urban traffic management.

In order to provide pedestrians and cyclists a safer environment, Taipei City government has been implementing the bike lane network plan since 2014. Considering the departure efficiency, that is, the time needed to eliminate the queue at traffic signals, three north-south arterials and three east-west arterials are selected. Each of them has a width of at least 40 meters and metro routes passes through four of them. The planned network is shown in Figure 1.1. For those with wider sidewalks, for example, Jen-Ai road and Zhong-Shan N. road, marking lines for bike lanes are painted on the original sidewalks. For the other four routes, sidewalks are first broadened, and then marking lines

2

are drawn. The layout of a widened sidewalk with a bike lane is shown in Figure 1.2.

Residents had been reporting the congestion and inconvenience during the bike lane construction on Fu-Xing S. Road and Xin-Sheng S. Road from March to September in 2016. According to the travel speed collected from vehicle detectors, during the construction, travel speed slightly decreased by 6.49% to 7.91% and the service level had been degraded (Taipei City Traffic Engineering Office, 2016). However, the service level had almost recovered after the construction work was completed. Hence, whether there are some differences in terms of the traffic flow characteristics and congestion propagation pattern between arterials under construction and the others is worth investigating. Moreover, more detailed understanding of relationships among neighboring road segments may also provide traffic management agencies and individuals valuable information for evaluating the influences of construction decisions, determining traffic management strategies and providing navigation. Hence, high-resolution VD data during the construction in an ROI covering the arterials under construction can be extracted for further analysis. Characteristics of the congestion propagation pattern including the conditional probability that a congestion may occur given the occurrence of another congestion, the potential relationship between adjacent road segments and how traffic congestion contribute to different road segments can be observed.
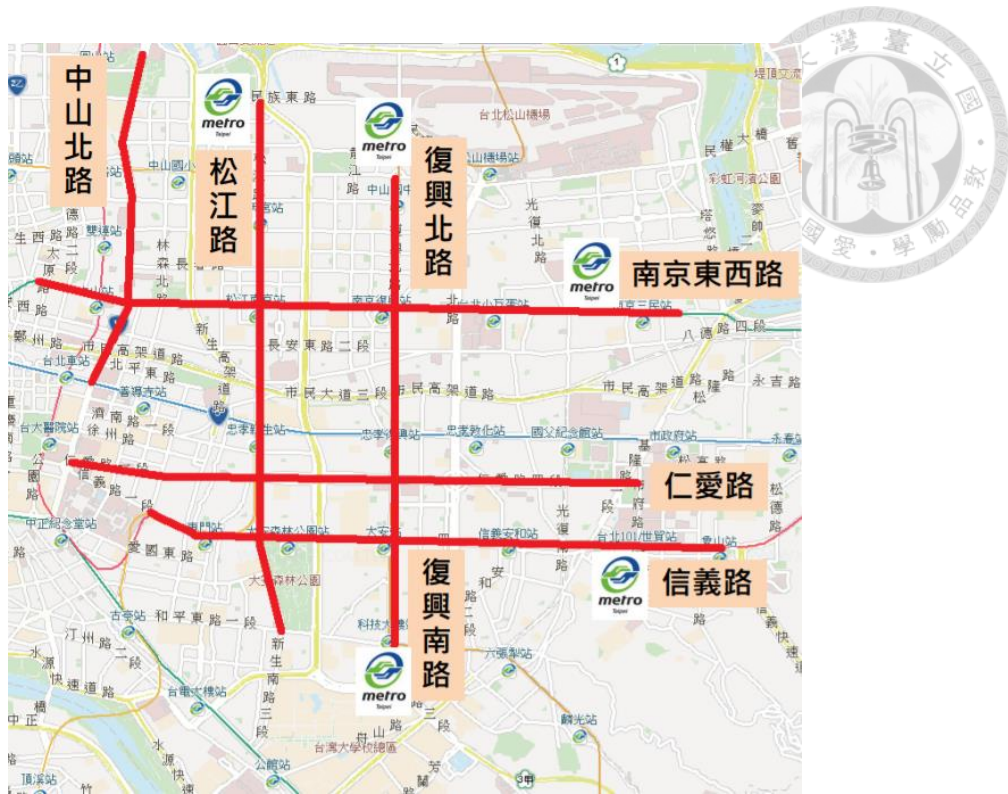
Figure 1.1 Planned Bike Lane Network in Downtown Taipei

Figure 1.2 Layout of Widened Sidewalk on Fu-Xing S. Road

4

In this study, we seek to obtain better understanding of the pattern of how traffic congestion propagates and influences a roadway network. The traffic control center of Taipei City has provided a system for real time traffic status inquiry by plotting the road performance information on a Google Map as partly shown in Figure 1.3. Straightforward information can be extracted based on the collected traffic data (Chen, Guo & Wang, 2015), while the cascading traffic pattern may further suggest driver behavior of diverting to circumvent congested road segments. Hence, the main purpose of this study is to go deeper to investigate the effects of congestion afterwards. To monitor where and when traffic congestion occurs, we take point vehicular speed as the primary consideration. Based on the traffic data collected from vehicle detectors (VDs), we cluster these data by capturing the spatiotemporal variation of vehicular speed over the network so as to identify congestion incidents. Based on the congestion incidents identified, affected road segments can also be further determined.
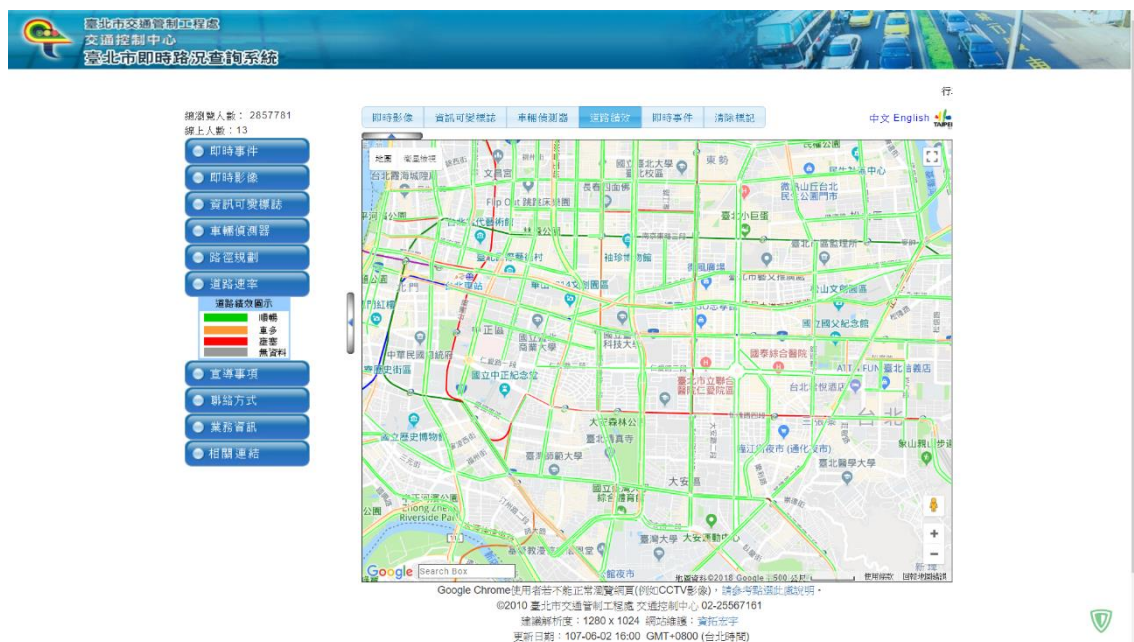
Figure 1.3 Real Time Traffic Status of Taipei City

5

Ultimately, this research seeks to investigate the propagation of congestion incidents within an urban road network. By visualizing the bottle necks and shockwave after a congestion occurs, we provide some research insight so that a precautionary traffic management strategy may be taken.
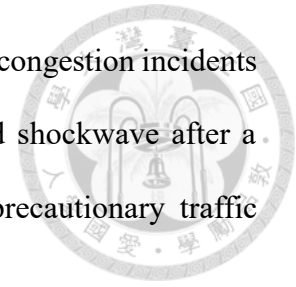
1.2 Research Objectives

In this study, we expect to have further understanding about the cascading pattern of traffic congestion based on high resolution VD data, which may be a reference for the determination of traffic management strategies. System for real time traffic status inquiry provided by the traffic control center of Taipei City and Google Map visualize instant traffic status in terms of vehicular speeds over the roadway network via a web-based inquiry interface, but we are more interested in the probability of congestion passing to neighboring areas. To be more specific, the research objectives are summarized as below:

I. Propose an alternated probability density estimation approach to properly compute the conditional probability that a congestion may occur on a certain road segment given the occurrence of another congestion.

II. Determine the potential relationship between adjacent road segments based on the degree of adjacency and turning (straight, left turn or right turn) pattern.

III. Visualize the density estimation result and discuss how a congestion on a road segment make contributions to adjacent road segments and affect neighboring areas.

1.3   Thesis Organization

Figure 1.4 illustrates the organization of this thesis, which consists of six chapters. Chapter 2 provides the literature review of several dimensions related to traffic states and events detection, propagation patterns of congestion and the applications of different forms of Kernel Density Estimation (KDE) approaches. Based on the gaps identified in Chapter 2, Chapter 3 proposed an alternated form of KDE approach, descriptively presented the associated data used for analysis and showed the procedure to apply the proposed approach. Next, Case studies using the road network of Taipei City are performed, and results are visualized in Chapter 4. Finally, conclusions of research findings and recommendations for future research are summarized in Chapter 5.
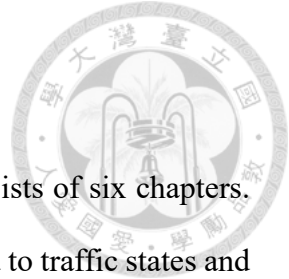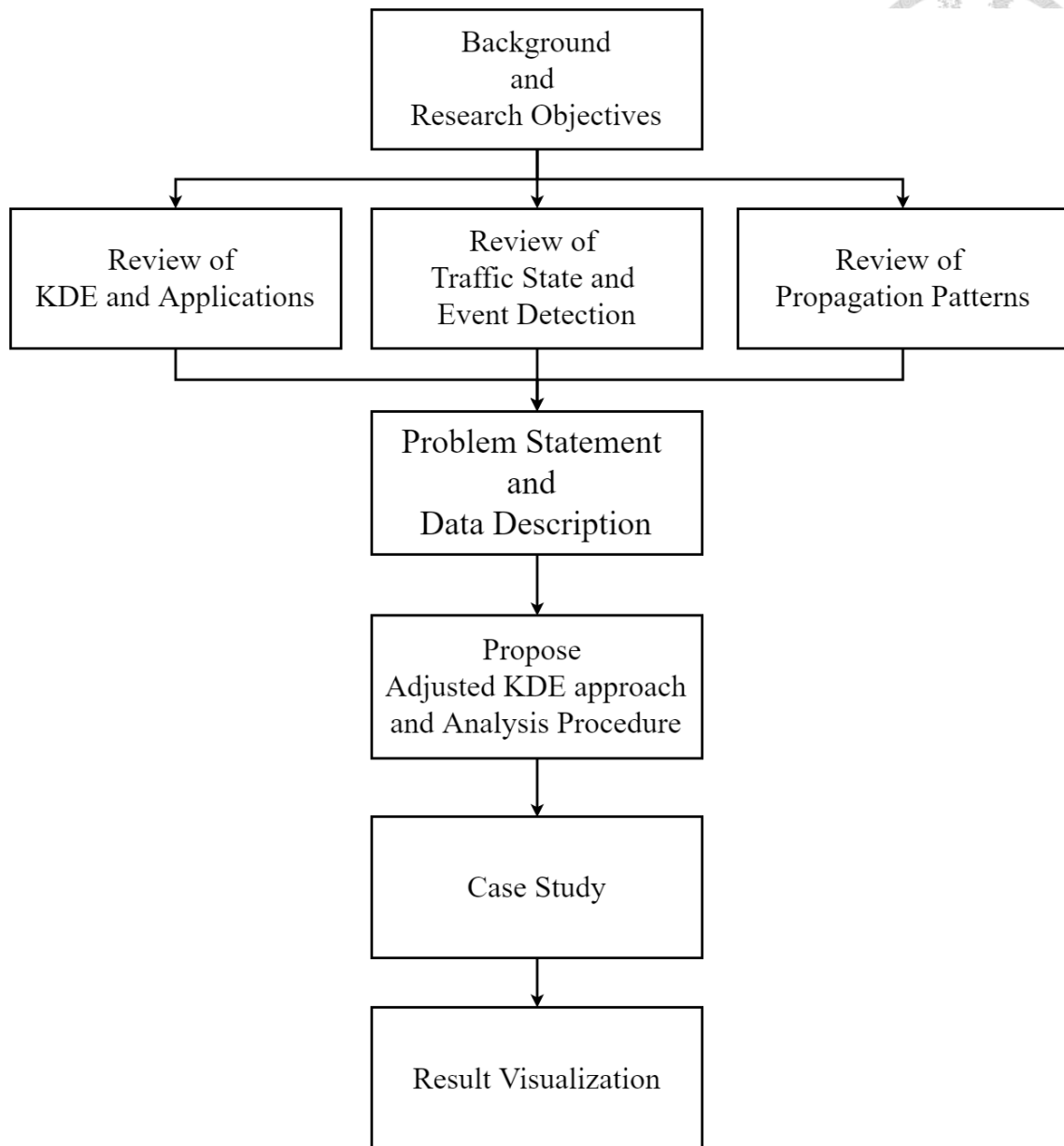
Figure 1.4 Thesis Organizations

Chapter 2 Literature Review
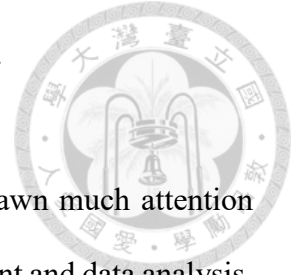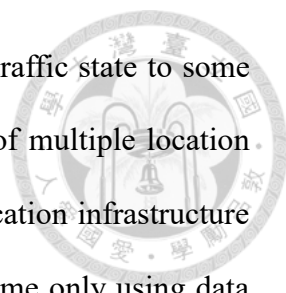
The situation of traffic congestion within road network has drawn much attention from both governmental and private units related to traffic management and data analysis. As detectors and monitors with high density installed and abundant traffic data collected, the insight into potential patterns within have intrigued increasing research interest to various case studies. These may lead us to further understanding to the characteristic of traffic flow, structure beneath our road network and some thoughts toward traffic management strategies.

This chapter will be organized as follows. The research papers applying different approaches for detecting traffic state and events are reviewed in section 2.1. Literature discussing the propagation pattern of traffic congestions is reviewed in section 2.2. Section 2.3 review the studies about kernel density estimation itself and its application in various disciplines. Last, a brief summary is presented in section 2.4.

2.1   Traffic State and Event Detection
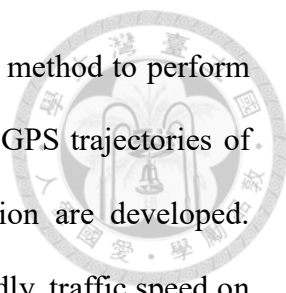
Congestion, slow, smooth and accidents are traffic states than can describe traffic flow on roads, providing critical information to travelers as well as transportation agencies (Li, She, Luo & Yu, 2013). Various data are collected from loop detectors, camera surveillance systems, probe cars and GPS including travel time, traffic speed and trajectories are used for traffic state and event detection. Algorithms are designed and case studies are performed on freeways and in urban road networks.

Coifman, B. (2002) stated that the link travel time can reflect traffic state to some extent. Direct measurement of travel time may require correlation of multiple location observations, that is, additional detector hardware or new communication infrastructure are needed. Thus, a method estimating trajectories and link travel time only using data from an individual set of dual loop detector is proposed. Basic traffic flow theory is applied for extrapolating local conditions on extended links. With no incidents or delays involved, this approach provides good time estimation results.

Kerner, Demir, Herrtwich, Klenov, Rehborn, Aleksic & Haug (2005) introduced an approach which perform traffic state detection with floating car data (FCD). Probe cars are sent to collect travel time within a reporting section. A travel time increase due to congestion emergence and a travel time decrease because of congestion dissolution are recorded. Two or more probe cars can provide substantial information for a typical traffic accident to be recognized. This approach can provide a 65% probability to recognize incidents last longer than 20 minutes with a penetration rate of 1.5% of probe cars within whole amount of vehicles.

Li, She, Luo & Yu (2013) applied freeway video surveillance system for traffic state detection use. Existing surveillance camera infrastructure can provide data in a video form. However, there are difficulties including angle and zooming while extracting traffic data form surveillance cameras. Based on the movement of vehicles in images, they proposed a system to estimate traffic flow speed and occupancy rate and estimate typical traffic states (congested, slow and smooth) that can leverage the existing surveillance infrastructure. The traffic state detection accuracy ratio during daytime is higher than 85%, while the accuracy of congestion reaches 91.8%.

10
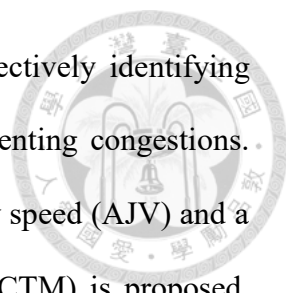
Wang, Lu, Yuan, Zhang & Van De Wetering (2013) proposed a method to perform visual analysis of urban traffic traffic jam based on trajectory data. GPS trajectories of taxis are collected and strategies for extract congestion information are developed. Trajectories are cleaned first in order to fit in a road network. Secondly, traffic speed on each road segment is calculated. Lastly, spatio-temporal graphs showing congestion and its propagation can provide descriptions of a traffic jam.

Anbaroglu, Heydecker & Cheng (2014) stated that differences between urban network and motorways, and the fact that the nature vary from recurrent congestions (RC) and non-recurrent congestions (NRC), limits the use of existing incident detection methods mostly focused on motorways without distinguishing RCs and NRCs. Substantially high link journey travel time observations (LJTs) occur simultaneously are clustered in the proposed NRC detection method. Besides minimum duration restrictions, localization index is also introduced to describe the closeness between congestion clusters. They concluded that those LJTs at least 40% higher than expected value should belong to NRC through the result of sensitivity analysis using a weighted product model (WPM).

2.2   Propagation Patterns

Besides detection of traffic states and events, how the congestion propagates and/or cascade is also one of the most interested issues among research related traffic congestion. This may provide us the ability to extrapolate the traffic state on the road network nearby and the potential relationship between neighboring road segments. With these we can further understand the structure of our road network and the cascading behavior of a congestion took place.
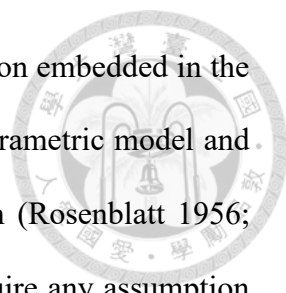
Long, Gao, Ren & Lian (2008) stated the importance of effectively identifying network bottlenecks for improving network service level and preventing congestions. Congestion is defined by critical standards based on average journey speed (AJV) and a congestion propagation model based on cell transmission model (CTM) is proposed. Simulations are performed on Sioux Falls network. The simulated result can provide references for decision in controlling traffic demand.

Wang, Z., et al. (2013) utilized GPS trajectories and provide multiple views for visually exploring and analyzing on the level of propagation graphs and road segment level. The whole visualization contains speed variation on pixel level while the propagation result is shown on road segment level.

Ji, & Geroliminis (2014) observed congestion propagation on a macroscopic scale. By taxi GPS as sparse probe vehicle data and maximum connected component of congested links, interconnected congested links and the critical congestion pockets are identified. The proposed method can effectively distinguish the congestion pockets out of the network and track the evolution of congestion through time.

2.3   Kernel Density Estimation (KDE) and Applications

An adjusted kernel density estimation approach is applied in this study, thus related literatures including the general kernel density estimation method and some discussion about this approach as well as the applications in transportation field and several other disciplines are reviewed in this section. Probability density estimation approaches can be categorized into parametric and nonparametric ones. Parametric probability density

estimation is made based on the assumptions related to the distribution embedded in the data set. However, there can be larger gaps between the assumed parametric model and reality. As a nonparametric probability density estimation approach (Rosenblatt 1956; Whittle 1958; Parzen 1962), kernel density estimation does not require any assumption for the distribution of data points. This provides more flexibility and allows researchers to discover more characteristics beneath the data set such as such as its actual distribution. Hence, the great importance of kernel density estimation has shown in both theoretical and applied statistics fields. Rosenblatt, M. (1956) and Parzen, E. (1962) developed current form of kernel density estimation, which is also termed Parzen-Rosenblatt window method in some fields such as signal processing and econometrics.

Yu (2009) has done a study on KDE, investigating the most appropriate search bandwidth choice for six different probability distribution evaluated by mean integrated square error (MISE) and asymptotic mean integrated squared error (AMISE). Yu concluded that the KDE with variable search bandwidth can provide acceptable estimation results.

Xie and Yan (2008) suggested a network KDE method transformed from a standard planar KDE to fill the shortcomings while the problem is network based. The innovation of this research is to represent network space with lixel, which is the linear units of equal network length. This approach is tested with traffic accident data and road network in Bowling Green, Kentucky in 2005. This approach has the ability to solve the problem of overestimation of density values. The impacts on density calculation from different kernel functions and different search bandwidth are also investigated and found that search bandwidth brought the highest influence by controlling the smoothness of the spatial pattern.

13

Chang (2012) applied KDE and integrate data mining to assess common physiological indicators of multiple diseases. To estimate the probability of illness of patients being examined, KDE is applied to estimate the probability distribution of each common physiological indicator under different health condition.

Hu (2012) established an approach to analysis GPS trajectory and collected the trajectories of visitors in Yehliu Geopark. Possible spatial distribution of visitors within the park can be calculated through KDE. In addition, time factor is also taken into account to investigate the location of crowds and the spatial distribution of visitors. Ultimately, the density distribution of visitors within the park during different time period is simulated. The simulation result can be used to reconsider the space allocation and route design.

2.3.1 Standard Kernel Density Estimation (Standard KDE)

Assuming $(x_1, x_2, ..., x_n)$ is a univariate independent and identically distributed sample extracted from some distribution with an unknown density f, its kernel density estimator can be written as:

$$f_h(x) = \frac{1}{n} \sum_{i=1}^{n} K_h(x - x_i) = \frac{1}{nh} \sum_{i=1}^{n} K(\frac{x - x_i}{h}) \tag{2.1}$$

Where K is the kernel function which is a non-negative symmetric function and satisfies $\int K(u)du = 1$. Since K is a probability density function, f also has the characteristics of probability density function. In practice, several kinds of probability density function commonly selected as K are listed below:

14

I. Uniform (rectangular window):

$$K(u) = \frac{1}{2}, \text{ for } |u| \leq 1 \tag{2.2}$$

II. Triangular:

$$K(u) = (1 - |u|), \text{ for } |u| \leq 1 \tag{2.3}$$

III. Epanechnikov (parabolic):

$$K(u) = \frac{3}{4}(1 - u^2), \text{ for } |u| \leq 1 \tag{2.4}$$

IV. Quartic (biweight):

$$K(u) = \frac{15}{16}(1 - u^2)^2, \text{ for } |u| \leq 1 \tag{2.5}$$

V. Gaussian:

$$K(u) = \frac{1}{\sqrt{2\pi}} e^{-\frac{1}{2}u^2} \tag{2.6}$$

In Eq. (2.1), h is a positive number named bandwidth or smoothing parameter. It controls the smoothness and preciseness of kernel density estimation. A larger h may lead to underfitting and fail to represent the appearance of the real density function. By contrast, a smaller h does not perform well on smoothing the curve and may lead to overfitting.

15

2.3.2   Planar Kernel Density Estimation (Planar KDE)

In order to perform density estimation of various spatial related issues, the standard kernel density estimation concept is then extended to 2-D planes. The general form of the planar kernel density estimator in a 2-D space can be written as:

$$\lambda(s) = \sum_{i=1}^{n} \frac{1}{\pi r^2} k(\frac{d_{is}}{r}) \tag{2.7}$$

Where $\lambda(s)$ is the density at location s, d_{is} is the distance from point i to location s, and r is the bandwidth in Planar KDE. k is the kernel, modeled as a function of $\frac{d_{is}}{r}$ ratio. Instead of giving an equal weight to all points within bandwidth r, a distance decay effect is taken into account. That is, as the distance between a point and location s increases, that point is weighted less while calculating the overall density. Some commonly applied kernel functions used to account for the distance decay effect are expressed in an alternated form below (Gibin, Longley, & Atkindon, 2007; Levine, 2004):

I.   Gaussian function:

$$k(\frac{d_{is}}{r}) = \frac{1}{\sqrt{2\pi}} \exp(-\frac{d_{is}^{2}}{2r^2}) \text{, when } 0 < d_{is} \leq r \tag{2.8}$$

$$k(\frac{d_{is}}{r}) = 0 \text{, when } d_{is} > r$$

16

II. Quartic function (approximating Gaussian function):

$$k(\frac{d_{is}}{r}) = K(1 - \frac{d_{is}^2}{r^2}), \text{ when } 0 < d_{is} \leq r \tag{2.9}$$

$$k(\frac{d_{is}}{r}) = 0, \text{ when } d_{is} > r$$

To ensure that the basic assumption $\int k(u)du = 1$ is not violated. $\frac{3}{\pi}$ and $\frac{3}{4}$ are

common values chosen for scaling factor K.

III. Minimum variance function:

$$k(\frac{d_{is}}{r}) = \frac{3}{8}(3 - 5\frac{d_{is}^2}{r^2}), \text{ when } 0 < d_{is} \leq r \tag{2.10}$$

$$k(\frac{d_{is}}{r}) = 0, \text{ when } d_{is} > r$$

2.3.3 Network Kernel Density Estimation (Network KDE)
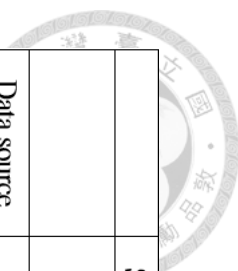
To perform density estimation of point events with network constraints, network

KDE is proposed (Xie & Yan, 2008). This approach differs from the planar kernel density

estimation in several aspects. Network KDE is a 1-D measurement, while planar KDE is

a 2-D one. Network space is used in the point event context and the kernel function is

developed based on network distance instead of Euclidean distance. Hence, it performs

better on density estimation while a planar KDE may over-detect clustered patterns. The

general form of the network KDE can be expressed as:

17

$$\lambda(s) = \sum_{i=1}^{n} \frac{1}{r} k(\frac{d_{is}}{r})$$

<div align="right">(2.11)</div>

2.4 Summary of Literature Review

The summary of characteristics of reviews in terms of data source, approaches and types of road network is listed in Table 2.1. According to the review in former sections, most studies focus on either traffic state and event detection or propagation patterns of congestions. Furthermore, there are some shortcomings on the data source they utilize. Some of them are not open to public while others require high operation cost and complicated preprocessing techniques. To bridge the gaps, this study proposed an adjusted KDE approach to account for congestion detection, propagation patterns and visualization of VD data.

Subject of study		Traffic state and event detection				Propagation patterns			
Author (Year)		Coifman (2002)	Kerner, B. S., et al. (2012)	Li, X., et al. (2013)	Anbaroglu, B., et al. (2014)	Long, J., et al. (2008)	Wang, Z., et al. (2013)	Ji, Y., et al. (2014)	This research
Data source	Probe car		✓						
	Surveillance system (camera)								
	Vehicle Detector	✓		✓	✓				
	Simulated								
	GPS trajectories					✓	✓	✓	✓
approaches	Traffic flow theory	✓							
	Communication model		✓						
	Image processing			✓					
	Spatio-temporal clustering								
	Cell transmission model					✓			
	Kernel density estimation								✓
	Visualization						✓	✓	✓
Types of road network	Urban road network		✓		✓	✓	✓	✓	✓
	Motorways	✓		✓					✓

Table 2.1 Summary of Characteristics of Reviews

19

Chapter 3 Methodology
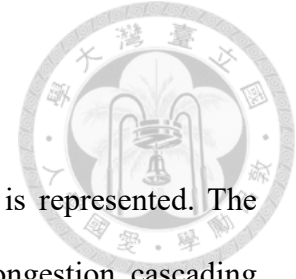
In this chapter, the characteristics of adjusted network KDE is represented. The proposed adjusted KDE approach is applied to determine the congestion cascading pattern in terms of the conditional probability for congestion incidents and the potential relationship between adjacent road segments is investigated. Procedures of extracting network information, preprocessing VD data and performing KDE estimation by employing the proposed approach are also explained in this chapter.

3.1 Adjusted Network Kernel Density Estimation (Adj. Network KDE)

In this study, we will make some adjustments on the original network KDE approach. In order to interpret the spatio-temporal characteristic of the congestion propagation within an urban road network, network kernel density estimation approach is applied. Instead of using network distance, this research employs "degree of adjacency" based on the structure of the road network and adjacency matrix. The locations of VDs do not follow a specific rule, for example at the front, middle or the end of the road segment. Hence, VD data can only present the whole road segment and precise network distance cannot be calculated. Furthermore, the conditional probability that congestion occurs on the upstream road segment given the occurrence of another congestion on the downstream road segment is also considered. The adjusted form of the network KDE can be written as:

20

$$\lambda(s) = \sum_{i=1}^{n} \frac{1}{r} p_{is} k(\frac{adj_{is}}{r})$$ (3.1)
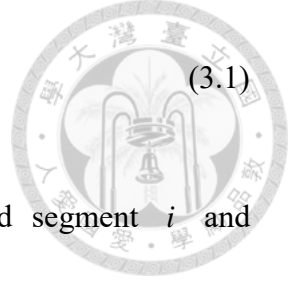
Where adj_{is} is the degree of adjacency of upstream road segment i and downstream road segment s and p_{is} is the conditional probability that congestion occurs on i given another congestion occurring on s. To be more specific, s and i are both locations of VDs. In addition, each s can also be viewed as the center of several neighboring road segments including itself, which contribute the effect to adjacent i s.

3.2   Data Description

Two main components of our data are introduced in the following sections, including the description of how we represent our urban road network structure, as well as the contents and the procedure of preprocessing raw VD data. We apply the conception of the adjacency matrix to form our road network structure. String comparison technique is applied to filter target VD set in our region of interest (ROI) and time intervals, while criteria are set to perform data preprocessing including the elimination of erroneous and some conversion of units.

3.2.1   Network Structure

The concept of the adjacency matrix is introduced to describe the network structure of our ROI. Most networks in previous research have been binary in nature. That is to say, the edges between nodes are either existing or not (Newman 2004). A network with such an attribute can be represented by an $n \times n$ adjacency matrix A with elements

$$A_{ij} = \begin{cases} 1 & \text{if } i \text{ and } j \text{ are connected,} \\ 0 & \text{otherwise} \end{cases}$$

However, our road network is slightly different. Since all the VDs are located on the road segments, our adjacency matrix is edge based. Furthermore, most of the arterials in our road network are bidirectional, and thereby the direction of traffic is also considered. That is, we will have an $n \times n$ adjacent matrix A where d is the entrance of a downstream road segment with respect to the exit of an upstream road segment u with elements

$$A_{du} = \begin{cases} 1 & \text{if } d \text{ and } u \text{ are connected,} \\ 0 & \text{otherwise} \end{cases}$$

Figure 3.1 shows a sample road network, while table 3.1 represents its 1st order adjacency matrix. We name it the 1st order adjacency when $A_{du} = 1$. The 1st order adjacent matrix of our ROI will be constructed following the conception of adjacency and part of it is shown in Figure 3.2. For some of the road segments, there are no VD installed. Another matrix containing the turning information is also constructed at this stage, as shown in Table 3.2. The tuning information is extracted from the VD reference data set, and the attribute is tagged as S (straight), L (left turn) and R (right turn). For those cannot be identified, coordinate information in terms of longitude and latitude is applied.

22
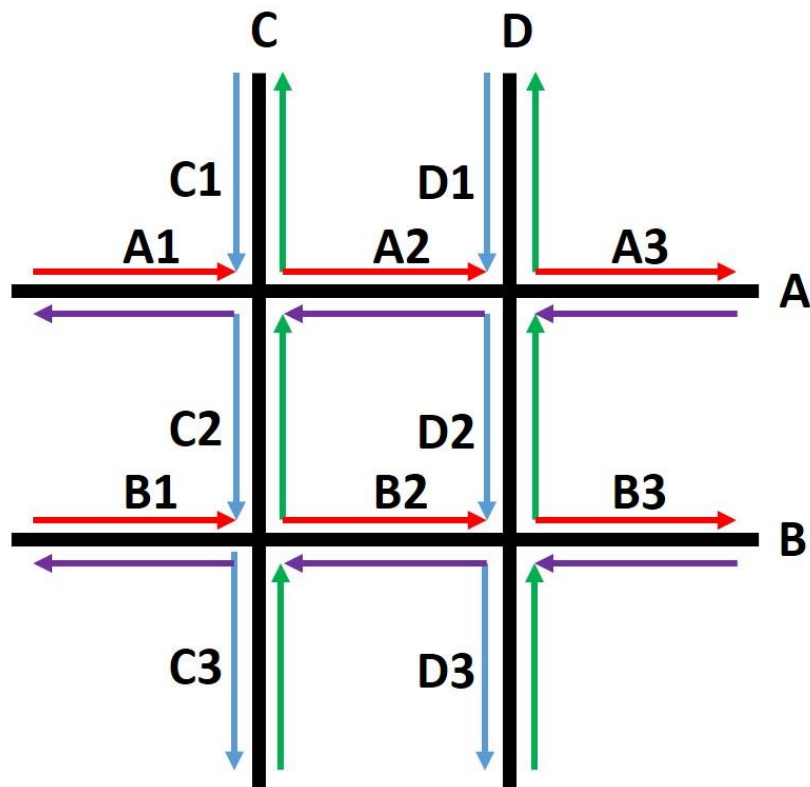
Figure 3.1 Road Network Example

Table 3.1 Adjacency Matrix Example

Downstream Arterial	ID	Direction	Upstream Arterial ID Direction Segment	A A2E East CD	B B2E East CD	C C2N North AB	D D2N North AB	... ...
A	A2E	East	CD	1	0	1	0	
B	B2E	East	CD	0	1	0	0	
C	C2N	North	AB	0	0	1	0	
D	D2N	North	AB	0	1	0	1	
…	…	…	…					…

23

編號	幹道	ID	方向	Bfrom(尾)→編號	0	1	2	3	4	5	6	7	8
				下游→幹道	信義	信義	信義	信義	信義	信義	和平東	和平東	和平東
Ato(頭)	上游			ID	VHSIP20	VHNJV20	VHMKV20	VHMM620	VHMML20			VFZK620	VG6J520
				方向	東	東	東	東	東	東	東	東	東
編號	幹道	ID	方向	路段	杭金	金新	新建	建復	復敦	敦光	南羅	羅金	金新
0	信義	VHSIP20	東	杭金	1	1	0	0	0	0	0	0	0
1	信義	VHNJV20	東	金新	0	1	1	0	0	0	0	0	0
2	信義	VHMKV20	東	新建	0	0	1	1	0	0	0	0	0
3	信義	VHMM620	東	建復	0	0	0	1	1	0	0	0	0
4	信義	VHMML20	東	復敦	0	0	0	0	1	1	0	0	0
5	信義		東	敦光	0	0	0	0	0	1	0	0	0
6	和平東		東	南羅	0	0	0	0	0	0	1	1	0
7	和平東	VFZK620	東	羅金	0	0	0	0	0	0	0	1	1
8	和平東	VG6J520	東	金新	0	0	0	0	0	0	0	0	1
9	和平東		東	新建	0	0	0	0	0	0	0	0	0
10	和平東	VFTLH60	東	建復	0	0	0	0	0	0	0	0	0
11	和平東		東	復敦	0	0	0	0	0	0	0	0	0
12	和平東	VFPMQ20	東	敦基	0	0	0	0	0	0	0	0	0
13	和平東		西	南羅	0	0	0	0	0	0	0	0	0
14	和平東	VFZK620	西	羅金	0	0	0	0	0	0	0	0	0
15	和平東	VG6J520	西	金新	0	0	0	0	0	0	0	0	0
16	和平東		西	新建	0	0	0	0	0	0	0	0	0
17	和平東	VFTLH60	西	建復	0	0	0	0	0	0	0	0	0
18	和平東	VFQM660	西	復敦	0	0	0	0	0	0	0	0	0
19	和平東		西	敦基	0	0	0	0	0	0	0	0	0
20	辛亥		東	汀羅	0	0	0	0	0	0	0	0	0
21	辛亥	VF9KB20	東	羅新	0	0	0	0	0	0	0	0	0
22	辛亥		東	新建	0	0	0	0	0	0	0	0	0
23	辛亥	VF9KW60	東	建復	0	0	0	0	0	0	0	0	0
24	辛亥	VEWM560	東	復基	0	0	0	0	0	0	0	0	0
25	辛亥	VDYN960	東	基芳	0	0	0	0	0	0	0	0	0
26	辛亥		西	汀羅	0	0	0	0	0	0	0	0	0
27	辛亥	VF9KB60	西	羅新	0	0	0	0	0	0	0	0	0
28	辛亥		西	新建	0	0	0	0	0	0	0	0	0
29	辛亥	VF9KW60	西	建復	0	0	0	0	0	0	0	0	0
30	辛亥	VEFMN20	西	復基	0	0	0	0	0	0	0	0	0
31	辛亥	VEFMN60	西	基芳	0	0	0	0	0	0	0	0	0
32	金山南	VIPIZ61	北	仁信	0	0	0	0	0	0	0	0	0
33	金山南	VJSJD40	北	信愛	0	1	0	0	0	0	0	0	0
34	金山南	VG8IK40	北	愛和	0	0	0	0	0	0	0	0	0
35	金山南	VIPIZ61	南	仁信	0	1	0	0	0	0	0	0	0

Figure 3.2 Part of the 1st Order Adjacency Matrix of Our ROI

Table 3.2 Turning Matrix Example
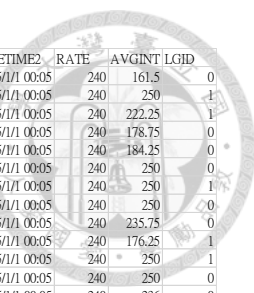
			Upstream Arterial	*A*	*B*	*C*	*D*	*...*
			ID	A2E	B2E	C2N	D2N	…
Downstream			*Direction*	East	East	North	North	…
Arterial	*ID*	*Direction*	*Segment*	CD	CD	AB	AB	…
A	A2E	East	CD	self	0	R	0	
B	B2E	East	CD	0	self	0	0	
C	C2N	North	AB	0	0	self	0	
D	D2N	North	AB	0	L	0	self	
…	…	…	…					…

This study focuses on the 1st and 2nd order adjacency, thereby requiring the 1st and 2nd order adjacency matrices and turning information. We make a dot product of the 1st order adjacency matrix itself to obtain the 2nd order adjacency matrix. In the 2nd order adjacency matrix, the elements with value 1, is named 2nd order adjacency. A 2nd order adjacency relationship indicates that two road segments are connected through another road segment.

3.2.2 VD data processing

The dataset contains high resolution VD data (recorded every 5 minutes) in Taipei City from January, 2015 to March, 2017, provided by the Traffic Control Center of Taipei City Traffic Engineering Office. Figure 3.3 shows part of the raw data. Some preprocessing work must be done in order to extract the target data we are interested in. The raw data contain information including device ID, date and time, lane order, volume and travel speed of large vehicles and regular passenger cars, lane occupancy, and average interval between vehicles. There are also columns for motorcycles, however, none of them are actually detected. Table 3.3 explains the important components in the VD data which are useful for this study. We use average travel speed as our major indicator for traffic congestion. The average travel speed is calculated by converting big car volume into car volume based on the passenger car unit. Travel speeds on different lanes within a road segment are averaged. In our analysis, data are filtered by ROI and the time interval of interest (different peak periods of weekdays).

25

DEVICEID	LANEORDER	BIGVOLUME	BIGSPEED	CARVOLUME	CARSPEED	MOTORVOLUME	MOTORSPEED	AVGSPEED	LANEOCCUPY	DATETIME2	RATE	AVGINT	LGID
VGUEI60	1	1	41	12	30.67	0	0	30.62	3.5	2015/1/1 00:05	240	161.5	0
VGUEI60	2	0	0	5	42	0	0	42	1.25	2015/1/1 00:05	240	250	1
VGUEI60	3	0	0	8	48	0	0	48	1.5	2015/1/1 00:05	240	222.25	1
VMEKQ40	0	0	0	13	44	0	0	44	2.25	2015/1/1 00:05	240	178.75	0
VMEKQ40	1	0	0	10	33.4	0	0	33.4	2.25	2015/1/1 00:05	240	184.25	0
VLMR820	0	2	63.5	1	0	0	0	42.33	0.75	2015/1/1 00:05	240	250	0
VLMR820	1	0	0	2	0	0	0	0	0.5	2015/1/1 00:05	240	250	1
VHWGD40	0	0	0	4	42.5	0	0	42.5	0.75	2015/1/1 00:05	240	250	0
VHWGD40	1	0	0	3	37	0	0	37	0.75	2015/1/1 00:05	240	235.75	0
VHWGD40	2	3	51	8	49.75	0	0	50.09	3	2015/1/1 00:05	240	176.25	1
VHWGD40	3	0	0	4	34	0	0	34	0.75	2015/1/1 00:05	240	250	1
VELJA00	0	1	40	0	0	0	0	21	0.5	2015/1/1 00:05	240	250	0
VELJA00	1	1	40	3	50	0	0	50	0.75	2015/1/1 00:05	240	236	0
VELJA00	2	0	0	6	37.67	0	0	37.67	1	2015/1/1 00:05	240	236	0
VELJA00	3	1	25	0	0	0	0	34	0.5	2015/1/1 00:05	240	250	0
VELJA00	4	0	0	7	40	0	0	40	1.25	2015/1/1 00:05	240	236.25	1
VELJA00	5	0	0	4	45	0	0	45	0.5	2015/1/1 00:05	240	224	1
VQFHC20	0	0	0	7	41.57	0	0	41.57	0	2015/1/1 00:05	240	41.5	1
VQFHC20	1	0	0	10	61.5	0	0	61.5	1	2015/1/1 00:05	240	32	1
VQFHC20	2	0	0	1	56	0	0	56	0	2015/1/1 00:05	240	14.75	1
VQFHC20	3	0	0	10	44.1	0	0	44.1	1	2015/1/1 00:05	240	32	1

Figure 3.3 Raw VD Data

Table 3.3 Contents of Columns

Columns	Contents
DeviceID	Name of vehicle detectors
DateTime2	Tag of date and time
LaneOrder	Number of lane
BigVolume	Volume of large vehicles
BigSpeed	Speed of large vehicles
CarVolume	Volume of regular passenger cars
CarSpeed	Speed of regular passenger cars
LGID	Identifier of the direction of traffic

There are slight differences between the two different procedures of preprocessing VD data in terms of the travel speed criteria setting. Level of Service (LOS) C and average speed are chosen in this study. The data preprocessing procedure is described as follows.

I. Filtering the data of the set of VDs based on our ROI and target time intervals by string matching techniques.

26

96 road segments and 66 VDs are included in our ROI. By unifying the time format of the raw data, string matching can be performed. Weekday data and weekend data are then separated.

II. Ignoring missing data and removing erroneous data due to malfunctioning VD devices.

Erroneous data here mean records whose values are obviously unreasonable. For example, travel speeds remain zero even during peak hours for several days or travel speeds exceeding the speed limit for over 40%.

III. Constructing the incident chart for different criteria respectively.

A. For LOS C, according to section 19.6 in 2011 Taiwan Highway Capacity Manual (Transportation Planning Division, 2011), travel speed can be used to determine LOS for urban road network with different speed limits. The complete criteria are shown in Table 3.4. We consider LOS C, which is often taken as the standard of light congestion by transportation management agencies as our threshold. Under this state, except for more restrictions in making lane changes, drivers and motorists also experience certain tension. In this study, a congestion is recorded if the travel speed is lower than 30 km/hr. The differences between the actual travel speed and the LOS C threshold are also calculated.

Table 3.4 LOS Criteria for Urban Road Network with 50km/hr Speed Limit

Average Travel Speed V (km/hr)	LOS
V≥35	A
30≤V<35	B
25≤V<30	C
20≤V<25	D
15≤V<20	E
V<15	F

B. For average speed, a different threshold is adopted. To detect non-recurrent incidents, the normal traffic condition should be defined so that we construct a baseline for reference first. The baseline is set based on the weekly average of travel speed within the week of the targeted time interval. The difference between the actual travel speed and the baseline value is calculated. Those lower than 80% of the value on the baseline are recorded.

IV. As a preparation step for further processing, data recorded from step III are transformed to a binary data structure. For negative values of the difference between the actual travel speed and the threshold, 1 is assigned for them, while others are assigned 0. The value 1 shows a VD detected a possible congestion or incident during a certain time interval, while 0 indicates an acceptable level of service.

3.3   Analysis Procedure

Base on the road network structure construction and data preprocessing, we can obtain the 1st order and 2nd order adjacency relationships of the road segments and binary incident chart of the VDs within our ROI. The analysis procedure will be explained as follows and shown in Figure 3.4.

I.   Detecting incidents

Base on the binary incident chart obtained from the data preprocessing stage, a cell with value 1 indicates possible congestion or incident takes place. For a single VD, if there is a sequence of value 1 that lasts for at least 4 time intervals (20 minutes), we define it as a possible congestion incident.

II.   Calculating the conditional probability that incidents occur on neighboring road segments p_{is}

Duration of each congestion incident is recorded in step I. During the congestion incident on a certain road segment, the numbers of consecutive time intervals identified as congested on neighboring road segments are also recorded. We define the ratio of the latter (upstream adjacent road segment) and the former (downstream road segment) as the conditional probability of neighboring road segments affected by the congested road segment.

III. Calculating the kernel density at each road segment

Based on the result in step II and adjacency relationship obtained from data preprocessing, the kernel density can be calculated through Equation (3.1). A simple example is provided for illustration as follows. For the road network shown in Figure 3.5, congestion occurs on the target road segment TG, road segment 1,R in the 1st order right turn relationship with respect to TG, and another road segment 2,SR in the 2nd order straight-right turn relationship with respect to TG. Two congestion incidents were detected on TG; one started from 6:45 AM and ended at 7:15 AM, while the other started from 8:20 PM and ended at 8:50 PM. Both lasted for six time intervals (30 minutes). How p_{is} of these two congestion incidents are obtained are shown in Figure 3.6(a) and Figure 3.6(b), respectively. 4 and 3 congestion intervals were detected on 1,R during the two congestion incidents on TG respectively. 3 and 3 congestion intervals are detected on 2,SR during the two congestion incidents respectively. Thus, the kernel density calculation is $\lambda(1,R) = \frac{1}{3}\frac{4}{6}k(\frac{1}{3}) + \frac{1}{3}\frac{3}{6}k(\frac{1}{3})$

for 1,R and $\lambda(2,SR) = \frac{1}{3}\frac{3}{6}k(\frac{2}{3}) + \frac{1}{3}\frac{3}{6}k(\frac{2}{3})$ for 2,SR if $r = 3$ is chosen as the search bandwidth.
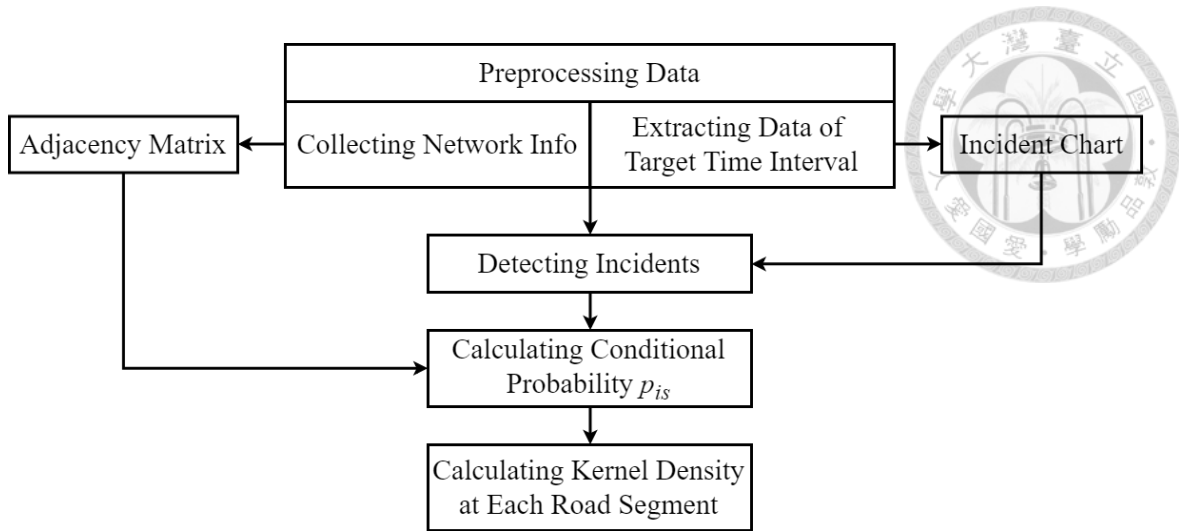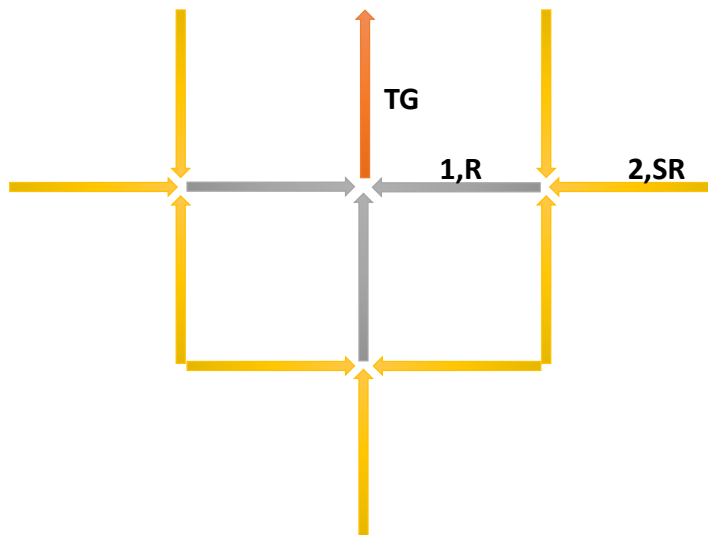
Figure 3.4 Analysis Procedure

Figure 3.5 Example Road Network for KDE

Interval / Segment	~6:50	~6:55	~7:00	~7:05	~7:10	~7:15	p_{is}
TG							
1,R							4/6
2,SR							3/6

Figure 3.6(a) p_{is} Calculation Example 1

31

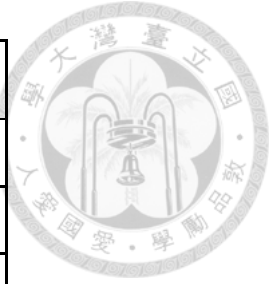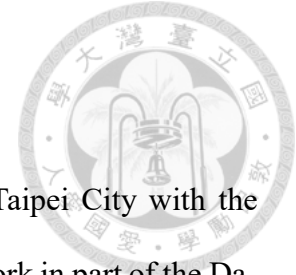| Interval Segment	~8:25	~8:30	~8:35	~8:40	~8:45	~8:50	p_{is}
TG							
1,R							3/6
2,SR							3/6

Figure 3.6(b) p_{is} Calculation Example 2

Chapter 4   Case Study

A case study is performed using the urban road network of Taipei City with the proposed algorithm applied. The dataset includes a real arterial network in part of the Da-an district, Taipei City. The VD data from January, 2015 to March, 2017 are provided by the Traffic Control Center of Taipei City Traffic Engineering Office. The point location of each VD is paired with a road segment. The network of our ROI is analyzed in this chapter in terms of the kernel density of congestion. Different scenarios, including a day with a special event and a week during the construction of bike lanes are investigated. The analysis for each scenario is organized as overview, segment-wise perspective and summary. The criteria of LOS C and average travel speed are analyzed, respectively.

4.1   Descriptions of the Case Study

Our ROI is defined by boundaries constructed by 5 arterials within Taipei City. The boundaries are listed in Table 4.1. The ROI area and locations of VDs installed are shown in Figure 4.1, where road segments are represented by thicker lines while the square dots represent VDs. Our ROI contains 96 road segments with different traffic directions separated. Totally 66 VDs are installed within this road network. There are no VDs on 30 road segments while multiple VDs are installed on some road segments. Data of peak hours during weekdays are extracted for analysis. VDs and their corresponding numbers and road segments are listed in Table 4.2.

33

Table 4.1 Boundaries of ROI

Boundary	North	South		West	East	
Arterial	Jen-Ai Rd.	1.	Xin-Hai Rd.	Hang-Zhou S. Rd.	1.	An-He Rd.
		2.	Roosevelt Rd.		2.	Le-Li St.

Figure 4.1 Road Network of the ROI and Location of VDs

Table 4.2 VDs in The ROI and Their Corresponding ID and Road Segments

ID	NO	Arterial	Dir	Block	ID	NO	Arterial	Dir	Block
VHSIP20	0	信義	東	杭金		16	和平東	西	新建
VHNJV20	1	信義	東	金新	VFTLH60	17	和平東	西	建復
VHMKV20	2	信義	東	新建	VFQM660	18	和平東	西	復敦
VHMM620	3	信義	東	建復		19	和平東	西	敦基
VHMML20	4	信義	東	復敦		20	辛亥	東	汀羅
	5	信義	東	敦光	VF9KB20	21	辛亥	東	羅新
	6	和平東	東	南羅		22	辛亥	東	新建
VFZK620	7	和平東	東	羅金	VF9KW60	23	辛亥	東	建復
VG6J520	8	和平東	東	金新	VEWM560	24	辛亥	東	復基
	9	和平東	東	新建	VDYN960	25	辛亥	東	基芳
VFTLH60	10	和平東	東	建復		26	辛亥	西	汀羅
	11	和平東	東	復敦	VF9KB60	27	辛亥	西	羅新
VFPMQ20	12	和平東	東	敦基		28	辛亥	西	新建
	13	和平東	西	南羅	VF9KW60	29	辛亥	西	建復
VFZK620	14	和平東	西	羅金	VEFMN20	30	辛亥	西	復基
VG6J520	15	和平東	西	金新	VEFMN60	31	辛亥	西	基芳
VIPIZ61	32	金山南	北	仁信	VINKW00	48	建國南	北	仁信
VJSJD40	33	金山南	北	信愛	VFVKW40	49	建國南	北	信和
VG8IK40	34	金山南	北	愛和		50	建國南	北	和辛
VIPIZ61	35	金山南	南	仁信	VINKW40	51	建國南	南	仁信
VJSJD40	36	金山南	南	信愛	VHMKW40	52	建國南	南	信和
VG8IK40	37	金山南	南	愛和		53	建國南	南	和辛
VINJW00	38	新生南	北	仁信		54	復興南	北	仁信
VFYKD00	39	新生南	北	信和	VHLM800	55	復興南	北	信和
VFYKD40	40	新生南	北	和辛1	VEWM500	56	復興南	北	和辛
VFYKD01	41	新生南	北	和辛2	VIAM700	57	復興南	南	仁信
VF9KB00	42	新生南	北	辛羅	VHLM800	58	復興南	南	信和
VINJW00	43	新生南	南	仁信	VEWM500	59	復興南	南	和辛
VFYKD41	44	新生南	南	信和	VI6NV00	60	敦化南	北	仁信

35

ID	NO	Arterial	Dir	Block	ID	NO	Arterial	Dir	Block
VFYKD40	45	新生南	南	和辛1	VGHN840	61	敦化南	北	信和1
VFYKD01	46	新生南	南	和辛2	VFNN700	62	敦化南	北	信和2
VF9KB00	47	新生南	南	辛羅		63	敦化南	北	和基
VI6NV00	64	敦化南	南	仁信	VDTJW00	80	羅斯福	南	舟基
VGHN840	65	敦化南	南	信和1	VCCKW00	81	羅斯福	南	基興
VFNN700	66	敦化南	南	信和2		82	基隆	北	汀羅
	67	敦化南	南	和基	VCPKT00	83	基隆	北	羅長
VGTHG00	68	羅斯福	北	杭和	VCZLY20	84	基隆	北	長辛
	69	羅斯福	北	和師		85	基隆	北	辛敦
	70	羅斯福	北	師辛	VF9NH00	86	基隆	北	敦和
VELJA00	71	羅斯福	北	辛新		87	基隆	南	汀羅
	72	羅斯福	北	新舟	VCPKT40	88	基隆	南	羅長
VDTJW00	73	羅斯福	北	舟基		89	基隆	南	長辛
VCCKW00	74	羅斯福	北	基興		90	基隆	南	辛敦
VGTHG00	75	羅斯福	南	杭和	VF9NH00	91	基隆	南	敦和
	76	羅斯福	南	和師		92	師大	北	和羅
	77	羅斯福	南	師辛		93	師大	北	羅汀
VELJA00	78	羅斯福	南	辛新		94	師大	南	和羅
VCPKT41	79	羅斯福	南	新舟		95	師大	南	羅汀

4.2 Result Analysis

The following result analysis is based on the kernel density estimation result of our ROI. Part of the kernel density estimation result of scenario 1 applying the criteria of average travel speed is shown in Table 4.3. For each ID, its adjacent road segments and their degree of adjacency are recorded and tagged as *adj_seg* and *degree*, respectively. The kernel density on each adjacent road segments of each day within the interested time interval are calculated respectively and then summed.

Table 4.3 Detailed KDE Result of Scenario 1 with Average Travel Speed

ID	adj_seg	degree	18	19	20	21	22	kdesum
1	33	1	0.2516	0.5032	0.1258	0.2516	0.3774	1.5096
1	35	1	0.2516	0.5032	0.1258	0.2516	0.3774	1.5096
1	0	1	0.1625	0.1761	0	0.1048	0.1931	0.6365
1	34	2	0.1375	0.1491	0	0.0887	0.1635	0.5388
2	43	1	0.2516	0.2516	0.2516	0.2516	0.2516	1.258
2	40	2	0.0776	0.1353	0.1331	0.1242	0.1531	0.6233
2	1	1	0.1205	0.097	0.0891	0.131	0.1022	0.5398
2	35	2	0.1154	0.1065	0.0754	0.1309	0.1043	0.5325
2	33	2	0.0799	0.0998	0.091	0.0865	0.1353	0.4925
2	39	1	0.0865	0.131	0.0446	0.0734	0.1232	0.4587
2	0	2	0.102	0.0821	0.0754	0.1109	0.0865	0.4569
2	8	2	0.0732	0.1109	0.0377	0.0621	0.1043	0.3882
2	16	2	0	0	0	0	0	0
3	51	1	0.629	0.629	0.629	0.5032	0.7548	3.145
3	17	2	0.5324	0.5324	0.5324	0.4259	0.6389	2.662
3	39	2	0.5324	0.5324	0.5324	0.4259	0.6389	2.662
3	49	1	0.3738	0.3124	0.1123	0.213	0.4031	1.4146
3	2	1	0.3414	0.2736	0.2361	0.3459	0.1999	1.3969
3	43	2	0.1597	0.2573	0.139	0.3347	0.3134	1.2041
3	1	2	0.289	0.2316	0.1999	0.2928	0.1692	1.1825
3	9	2	0	0	0	0	0	0
3	50	2	0	0	0	0	0	0
4	57	1	0.629	0.5032	0.5032	0.629	0.629	2.8934
4	18	2	0.5324	0.4259	0.4259	0.5324	0.5324	2.449
4	51	2	0.5324	0.4259	0.4259	0.5324	0.5324	2.449
4	3	1	0.2524	0.1866	0.2875	0.3649	0.3476	1.439
4	56	2	0.1982	0.2553	0.2571	0.3088	0.3117	1.3311
4	2	2	0.2137	0.1579	0.2434	0.3089	0.2943	1.2182
4	55	1	0.2831	0.2705	0.0252	0.2332	0.3008	1.1128
4	49	2	0.1445	0.1901	0.1597	0.2443	0.326	1.0646
4	10	2	0.2396	0.2289	0.0213	0.1974	0.2546	0.9418
7	75	1	0.1258	0.8806	0.5032	0.5032	0.7548	2.7676
7	6	1	0	0	0	0	0	0
7	69	1	0	0	0	0	0	0
7	70	2	0	0	0	0	0	0
7	93	2	0	0	0	0	0	0

4.2.1 Scenario 1: 2015/12/28~2015/12/31

The purpose of scenario 1 is to investigate the congestion propagation pattern during normal weekdays and a day with a special event, which is the New Year's celebration events in this case study. During this time period, the bike lane on Fu-Xing S. road and Xin-Sheng S. road was still under construction. The VD data from 12/28 to 12/31 in 2015 are extracted. The kernel density estimation of congestion is calculated for each road segments in our ROI.

Threshold of LOS C – Overview

The visualization of a KDE plain view is shown in Figure 4.2. Larger circle and darker color represents relatively higher density. Based on the threshold of LOS C (30km/hr), we can observe that the VDs with relatively high density are located on Xin-Sheng S. road, especially for the segment between the two largest arterials of Taipei City: Jen-Ai road and Xin-Yi road. For other road segments, generally they can still maintain level LOS C within peak hours. However, comparing Figure 4.2 with Figure 4.3 (for 12/31), only the color saturation at the locations of hot spots on the heat map become slightly higher, indicating higher probability of the occurrence of congestion.
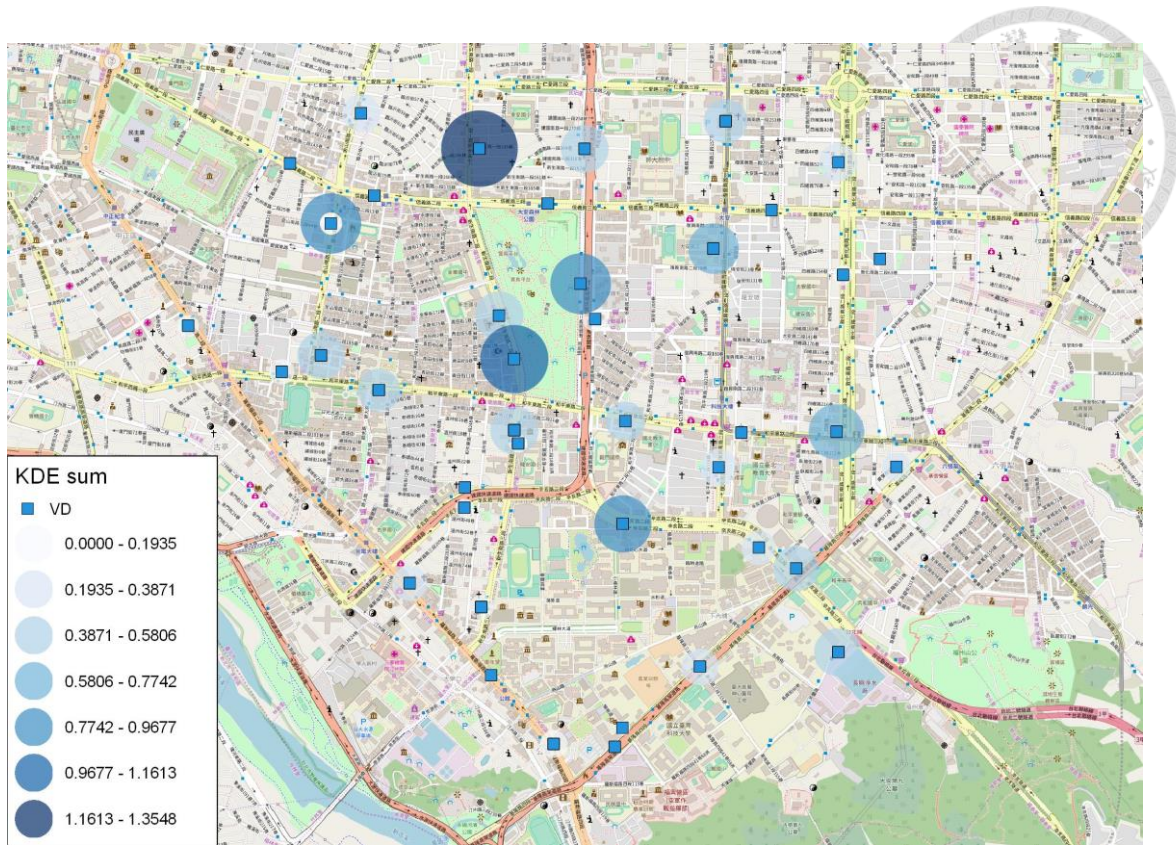
Figure 4.2 KDE of Scenario 1 with LOS C (2015/12/28~30)
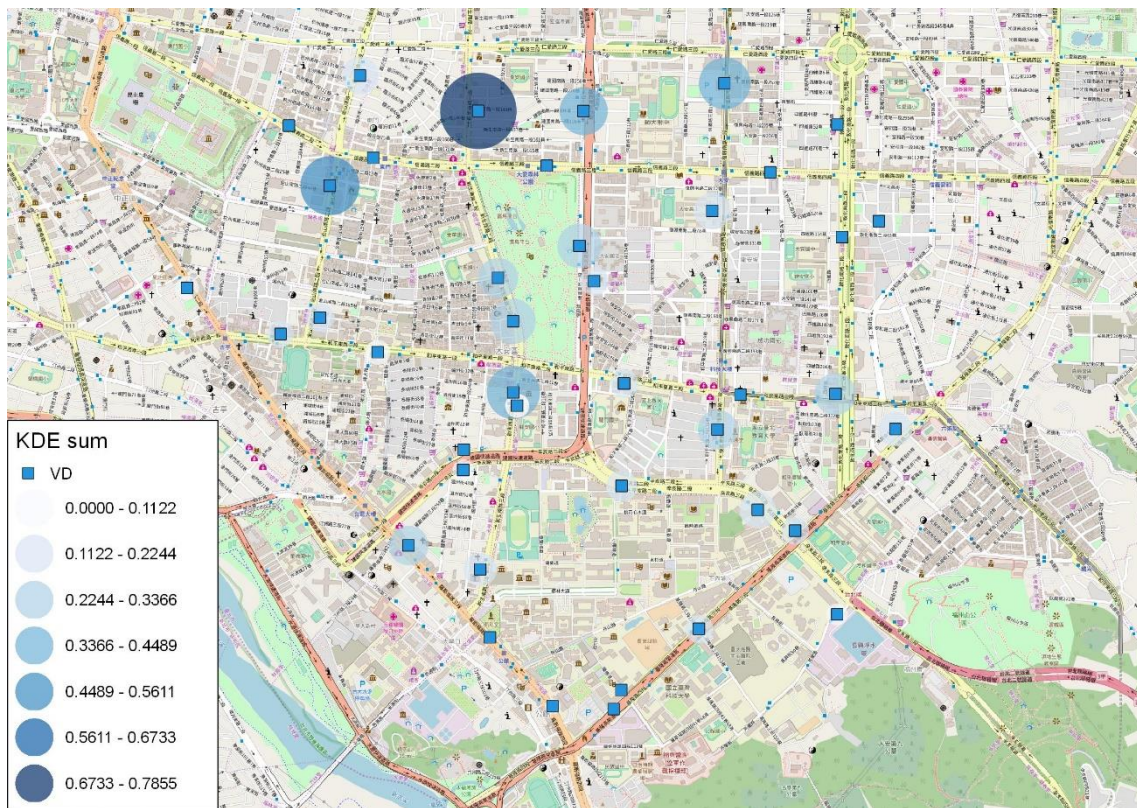
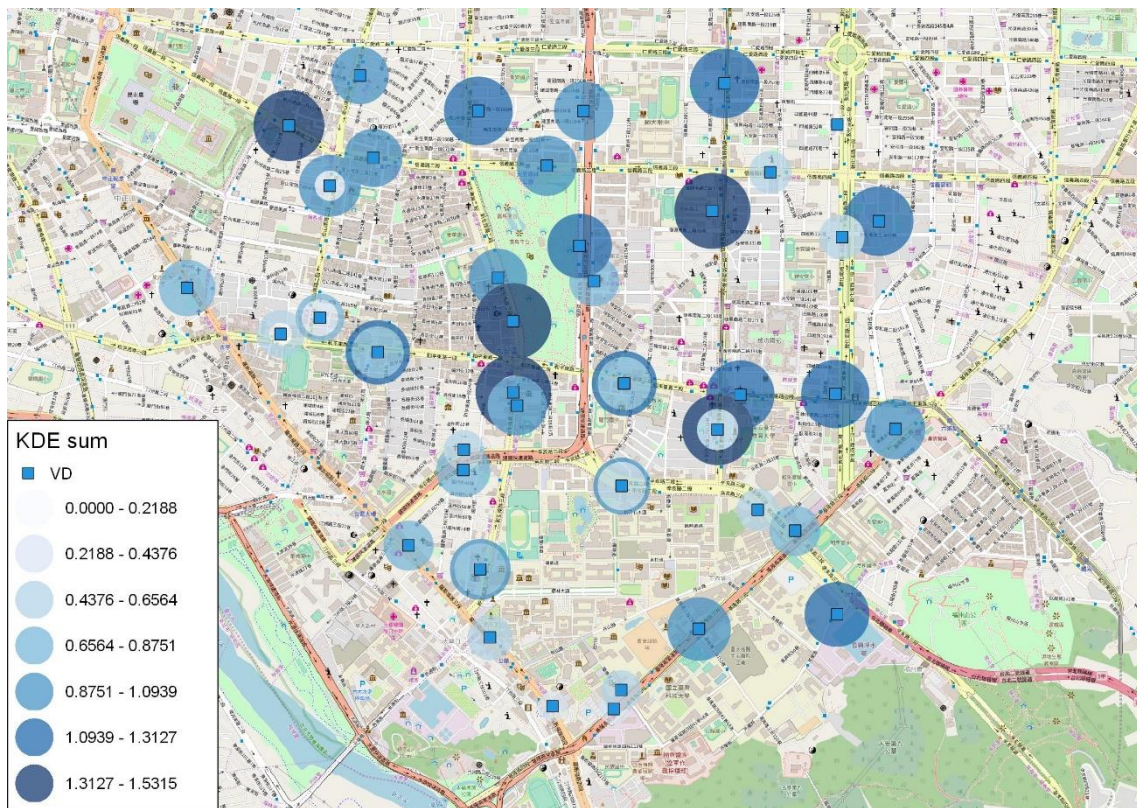Figure 4.3 KDE of Scenario 1 with LOS C (2015/12/31)

Threshold of LOS C - Segment-wise
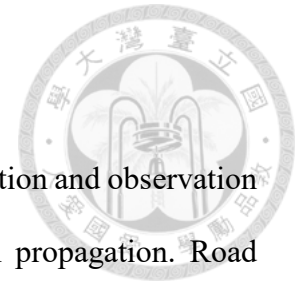
For road segments with relatively high density, further investigation and observation are needed, since they can be the potential sources of congestion propagation. Road segments 43 shows the highest density among all segments. However, since segment 43 is located at the north edge of our ROI, none of its upstream segments are accounted in this study. The possible congestion propagation to the upstream segments from the congestion of the origins of road segment 33, 43 and 44 is visualized in Figures 4.4, 4.5, and 4.6, respectively. The thickness and darkness of the color mark represents the degree of influence. Segments without a ramp can be either providing minor contributions or indicating the situation of no data obtained. The color red represents the congestion source road segments, while the upstream road segments are shown in gray scale. Darker color and thicker line segment indicates larger impact. White arrows indicate the travel directions.

For the analysis of road segment 33, the effect of congestion propagation to the upstream road segments are too minor to be observed.

For the analysis of road segment 44, road segments of the 1st order adjacency are more likely to be affected, while road segments of the 2nd order adjacency are influenced less. Among all road segments of the 2nd order adjacency, the one that enters road segment 44 by a left turn may be receiving more contribution from the congestion source.
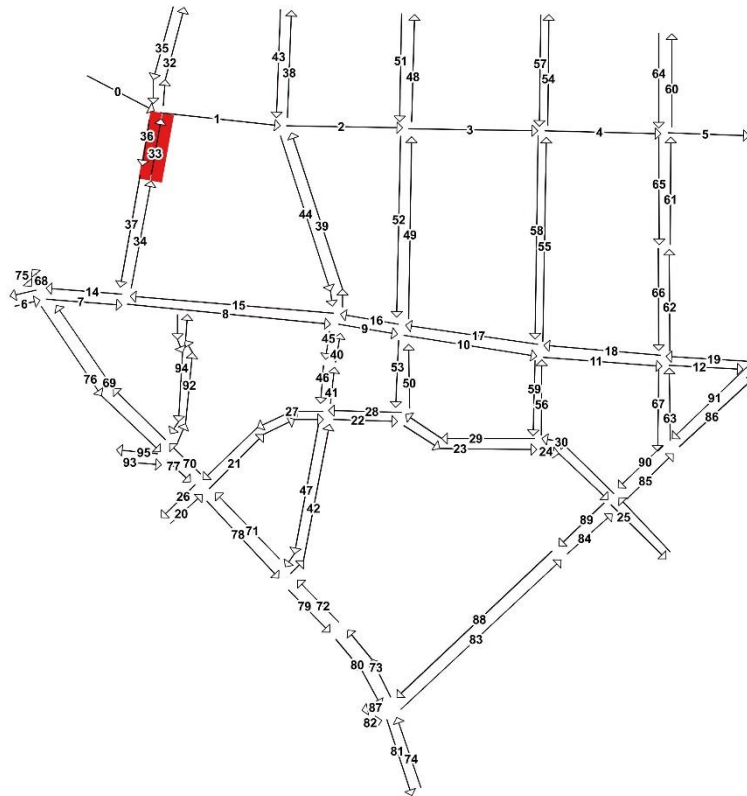
Figure 4.4 Upstream Influence from The Congestion of Segment 33 (S1_C)
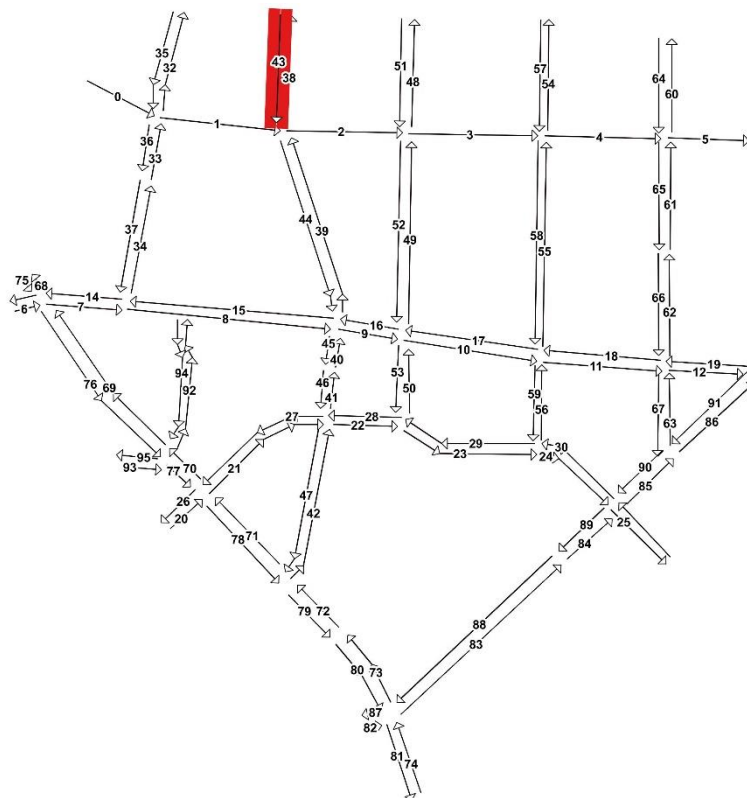
Figure 4.5 Upstream Influence from The Congestion of Segment 43 (S1_C)

41
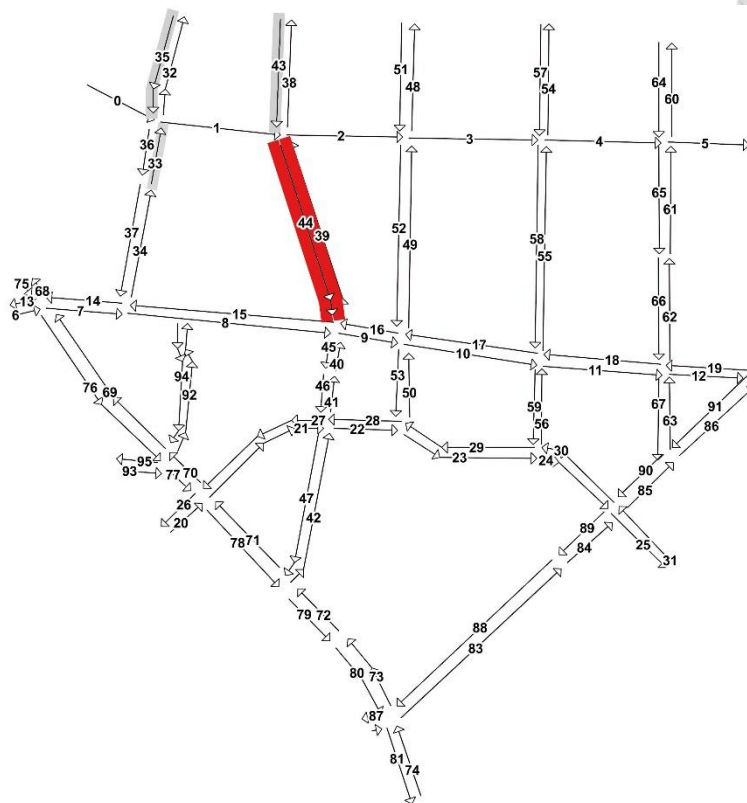
Figure 4.6 Upstream Influence from The Congestion of Segment 44 (S1_C)

Average Travel Speed - Overview

The visualization result presenting kernel density within the whole week of 2015/12/28 to 2015/12/31 is shown in Figure 4.7. Another figure specifically presenting the kernel density on 2015/12/31 is shown in Figure 4.8. The locations with larger circles and darker colors are road segments with higher kernel density. Similar locations of hot spots of congestion can be observed through Figure 4.7 and Figure 4.8. We can observe that the road segments on Xin-Sheng S. road, Jian-Guo S. road and Fu-Xing S. road near He-Ping E. road has relatively higher density than other road segments, indicating higher probability of the occurrence of congestion.

42
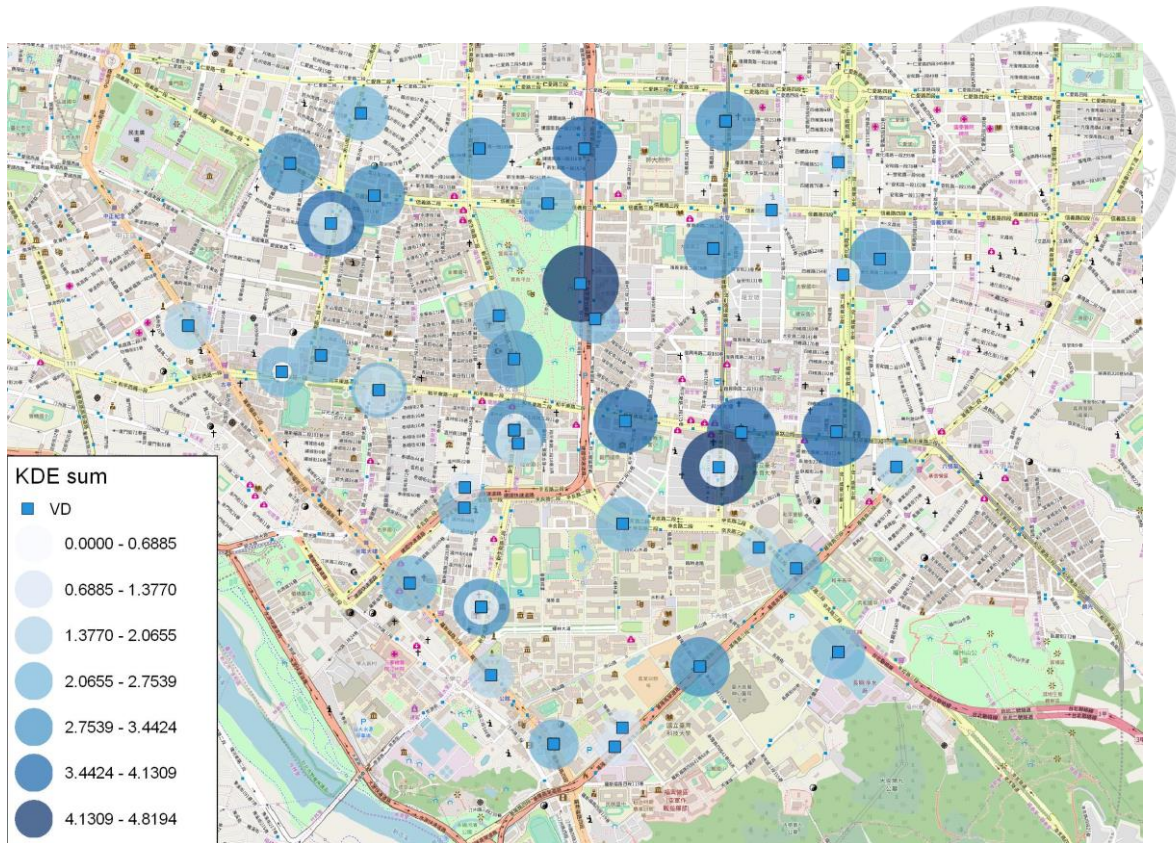
Figure 4.7 KDE of Scenario 1 with Average Travel Speed (2015/12/28~30)

Figure 4.8 KDE of Scenario 1 with Average Travel Speed (2015/12/31)

43

Average Travel Speed - Segment-wise

Road segments 40, 44 and 56 show the highest density among all segments. Hence, segment-wise analysis is performed. The possible propagation to the upstream segments from road segment 40, 44 and 56 is visualized in Figure 4.9, 4.10 and 4.11 respectively.

For the analysis of road segment 40, road segments of the 1st order adjacency are still more likely to be influenced. Road segments of the 2nd order adjacency are not affected as much as the road segment of the 1st order adjacency. Among those adjacent upstream road segments, the ones without a turn has higher density.

For the analysis of road segment 44, road segments of the 1st order adjacency are still more likely to be influenced. Since Xin-Yi road only allows one way traffic, there is no road segments entering road segment 44 by left turn. Among the two road segments of the 1st order adjacency, the effects are almost the same. Road segments of the 2nd order adjacency are not affected as much as the road segment of the 1st order adjacency. Among the three upstream road segments of the 2nd order adjacency, the effects are almost the same.

For the analysis of road segment 56, road segments of the 1st order adjacency are more likely to be affected. Among road segments of the 1st order adjacency, the one that enters by a left turn has higher density than the other that enters by a right turn. Road segments of the 2nd order adjacency following the road segment of the 1st order adjacency enter by a right turn are influenced less. Among all road segments of the 2nd order adjacency, the one does not enter by a left turn may receive more contribution to congestion from the source road segment 56 than the other.
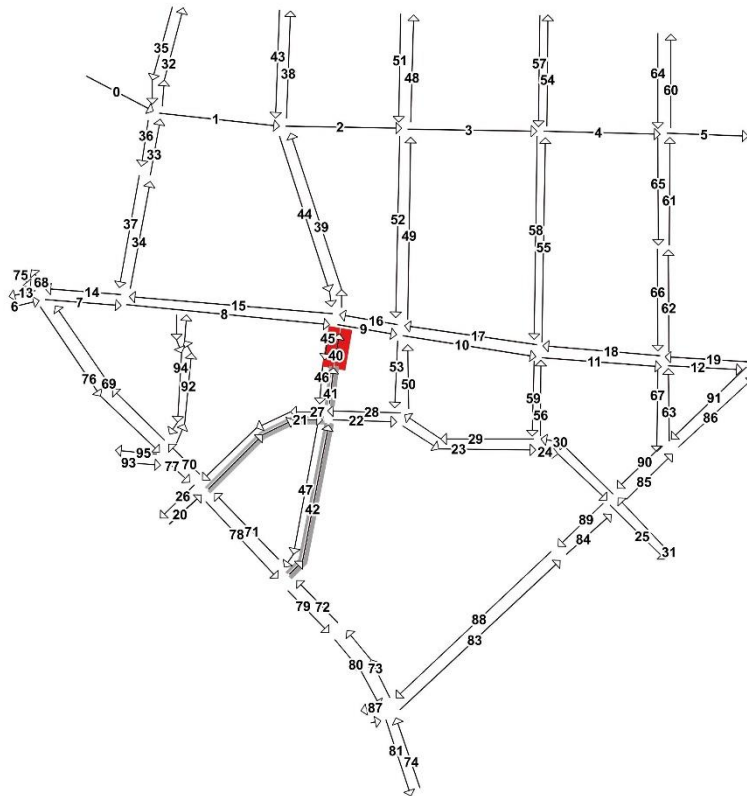
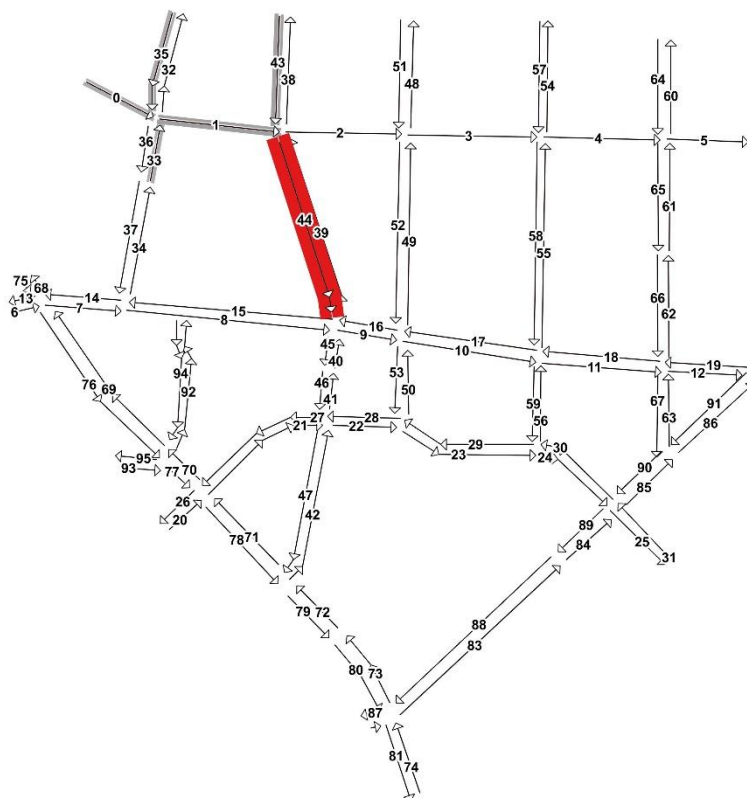Figure 4.9 Upstream Influence from The Congestion of Segment 40 (S1_avg)

Figure 4.10 Upstream Influence from The Congestion of Segment 44 (S1_avg)
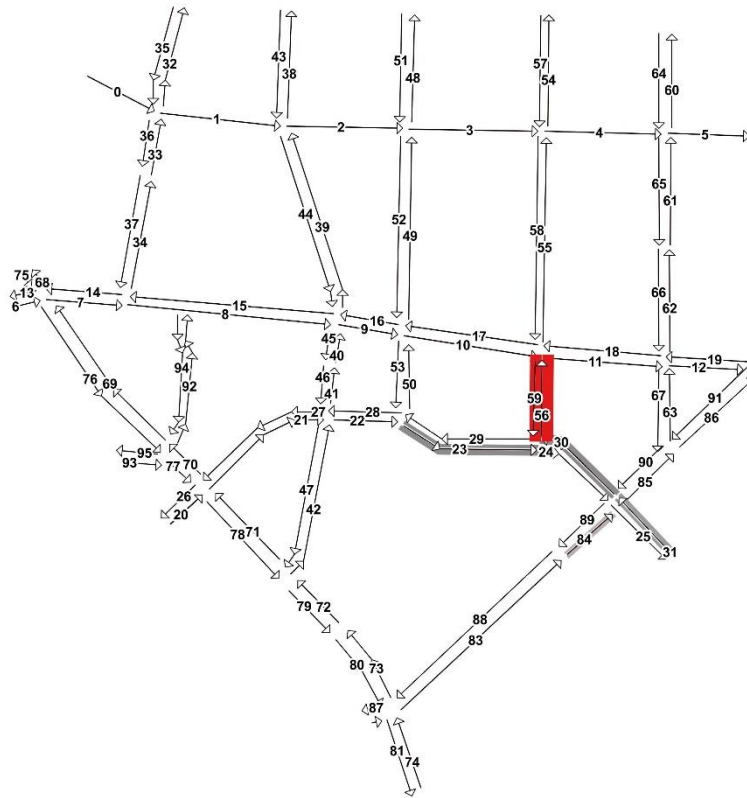
45

Figure 4.11 Upstream Influence from The Congestion of Segment 56 (S1_avg)

4.2.2   Scenario 2: 2016/4/18~2016/4/22

The construction of the bike lanes had caused occupation of lanes originally used by motorized vehicles and changed the layout of road segments. To investigate the congestion propagation pattern on weekdays during the construction of bike lanes, a week (2016/4/18 to 2016/4/22) during the construction and close to the completion of it is chosen for Scenario 2. Kernel density estimation is performed on each road segments in our ROI.

46

Threshold of LOS C – Overview
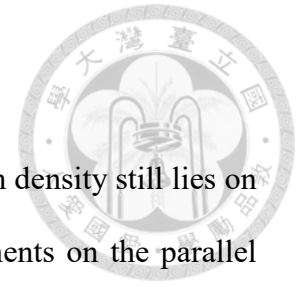
From the result shown in Figure 4.12, The main areas with high density still lies on Xin-Sheng S. road. However, the service level of some road segments on the parallel arterials including Jin-Shan S. road and Jian-Guo S. road may be degraded. The impact on the road segments seems to be more local, indicating that most of the congestions does not affect widely.
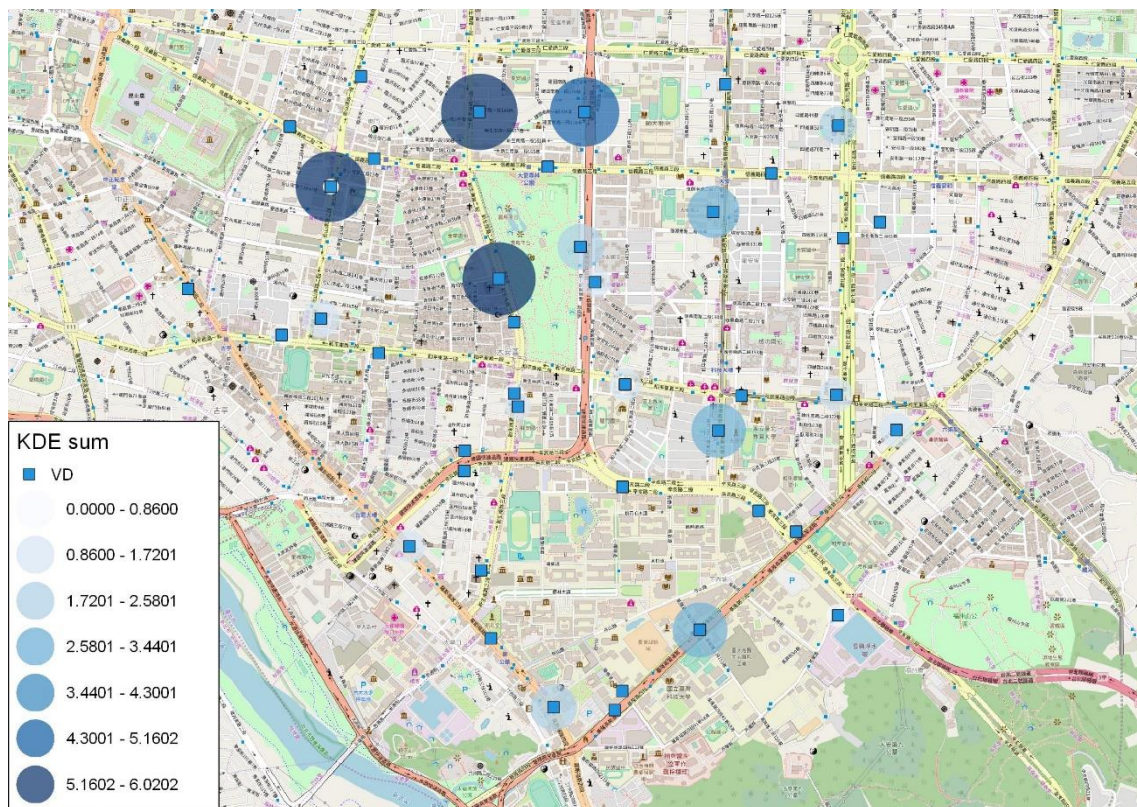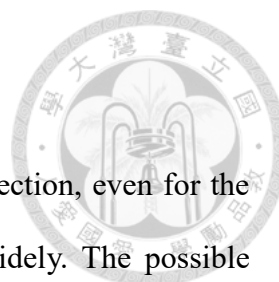

Figure 4.12 KDE of Scenario 2 with Level C of LOS (2016/4/18~22)

Threshold of LOS C - Segment-wise

Similar to what we have observed from the former overview section, even for the road segments with higher density, congestion does not spread widely. The possible congestion propagation to the upstream segments from the source of road segments 33, 39 and 84 is visualized in Figure 4.13, 4.14 and 4.15, respectively. Road segments 43 and 51 have higher density than road segment 84, however, their upstream road segments are not included in ROI.

In the analysis of the road segments for this period, the effect of propagation to upstream road segments is too minor to be observed.
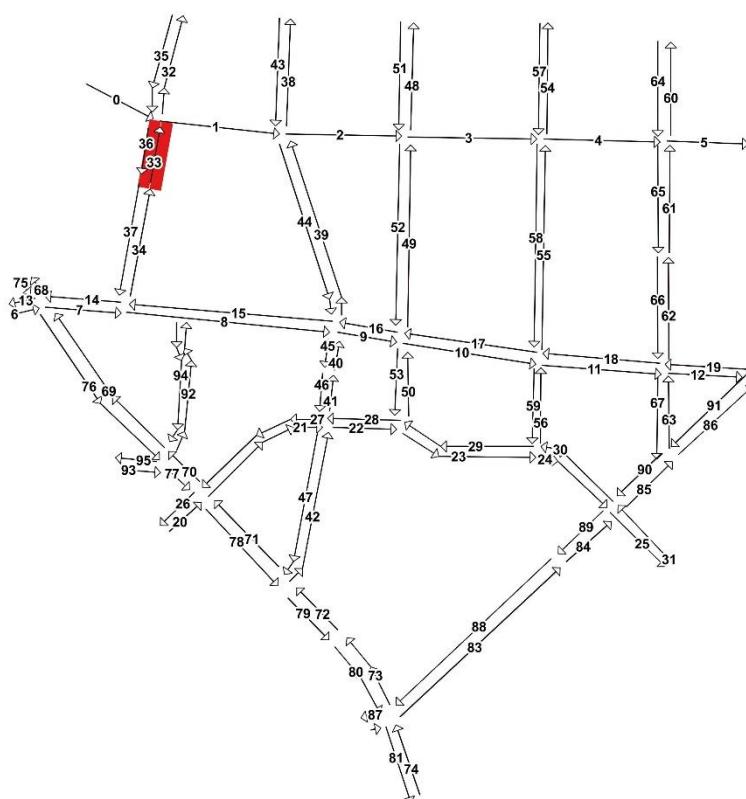
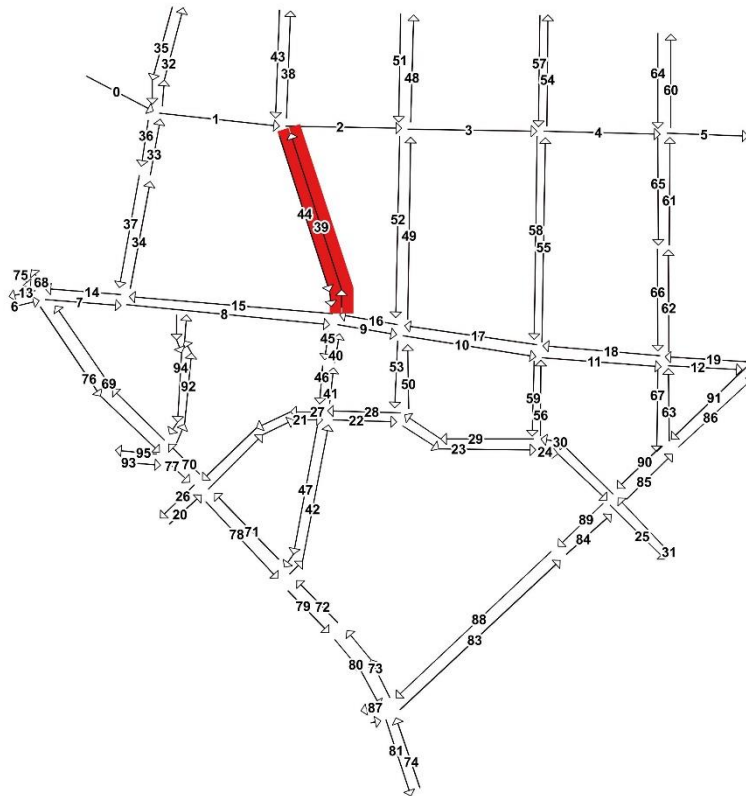Figure 4.13 Upstream Influence from The Congestion of Segment 33 (S2_C)

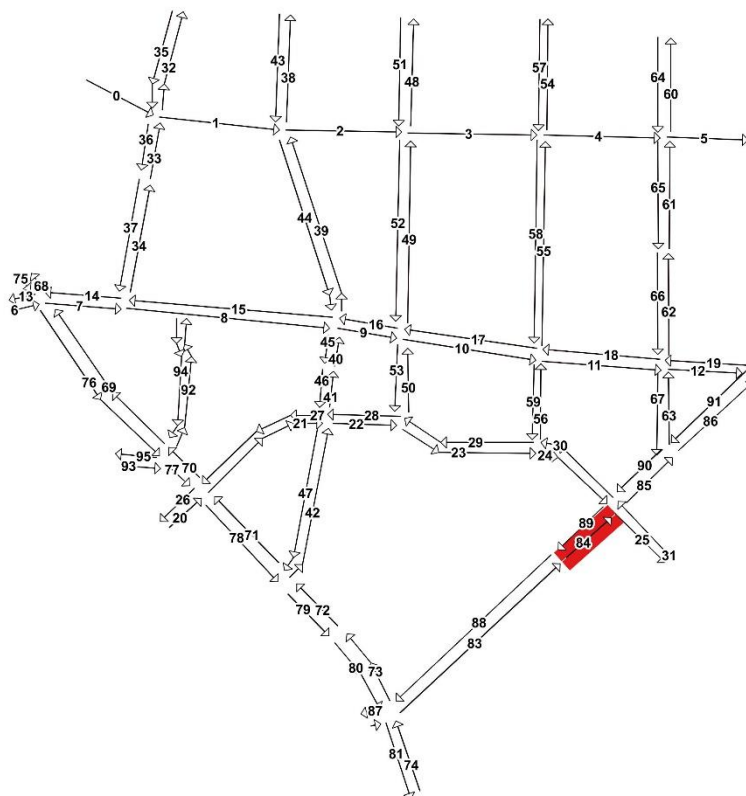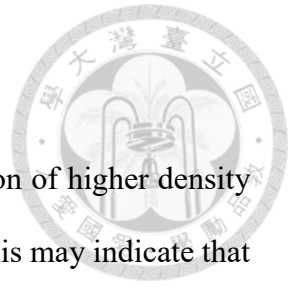Figure 4.14 Upstream Influence from The Congestion of Segment 39 (S2_C)

Figure 4.15 Upstream Influence from The Congestion of Segment 84 (S2_C)

49

Average Travel Speed – Overview

The visualization result is shown in Figure 4.16. The distribution of higher density areas is roughly unchanged, however, with lower color saturation. This may indicate that the impact from the construction has eased to some extent.
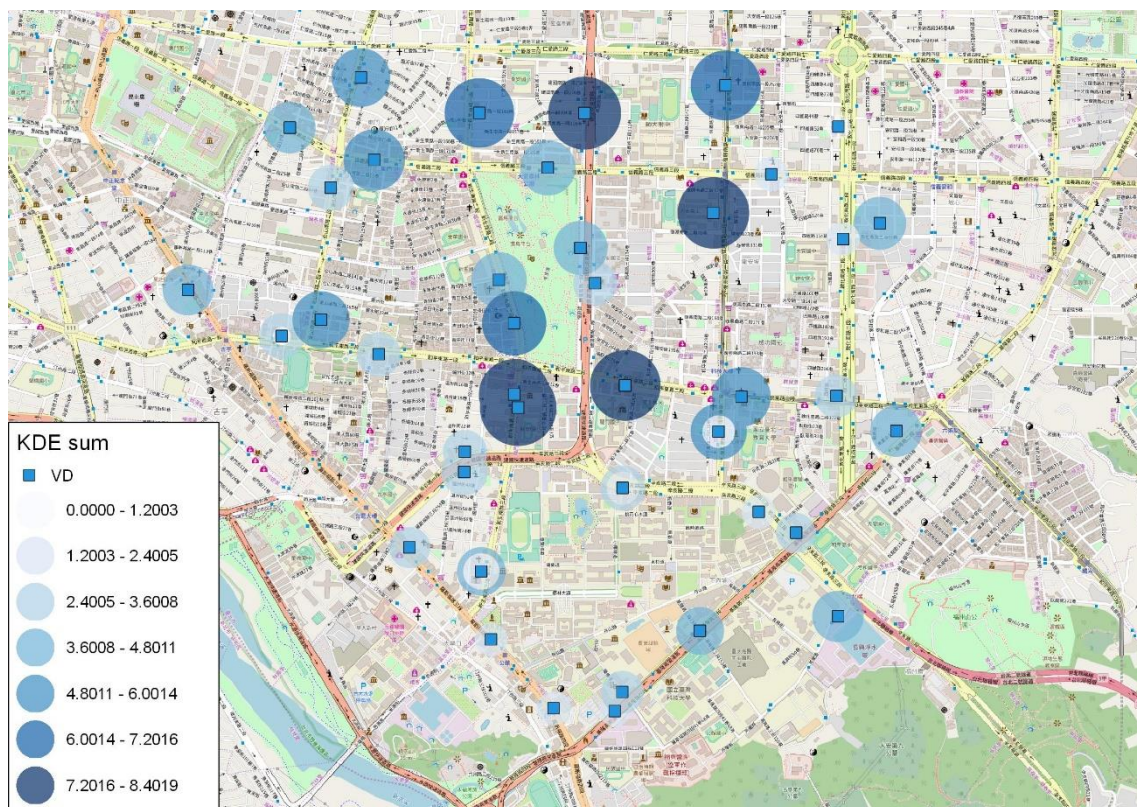

Figure 4.16 KDE of Scenario 2 with Average Travel Speed (2016/4/18~22)

Average Travel Speed - Segment-wise

Road segments 40, 46 and 51 show the highest density among all segments. However, the adjacent road segments of road segment 51 is not covered by ROI. The effects on road segment 58 with the 4th highest density is investigated and the pattern on road segment 56 is observed once again to compare with Scenario 1. The possible propagation to the upstream segments from the congestion of road segments 40, 46, 58 and 56 is visualized in Figure 4.17, 4.18, 4.19 and Figure 4.20, respectively.

For the analysis of road segment 40, there are one 1st order and two 2nd order adjacent upstream road segments. For the road segment of the 2nd order adjacency, the one that enters by a left turn has smaller density than the other one that enters without a turn and the road segment of the 1st order adjacency. However, the road segments of the 2nd order adjacent without turns has higher density than the 1st order adjacent one.

For the analysis of road segments 46 and 58, the effect of congestion propagation to upstream road segments are too minor to be observed.

For the analysis of road segment 56, similar patterns can be observed as they are in Scenario 1. Road segments of the 1st order adjacency are more likely to be affected. Among road segments of the 1st order adjacency, the segment that enters by a left turn has higher density than the other that enters by a right turn. However, the angle of the right turn here is about 135 degrees, its orientation may be defined between a right turn or a no turn. The road segments of the 2nd order adjacency entering the road segment of the 1st order adjacency by a right turn are influenced less. Among all road segments of the 2nd order adjacency, there are no significant difference between them in terms of the possible contribution to congestion received from the source road segment 56.
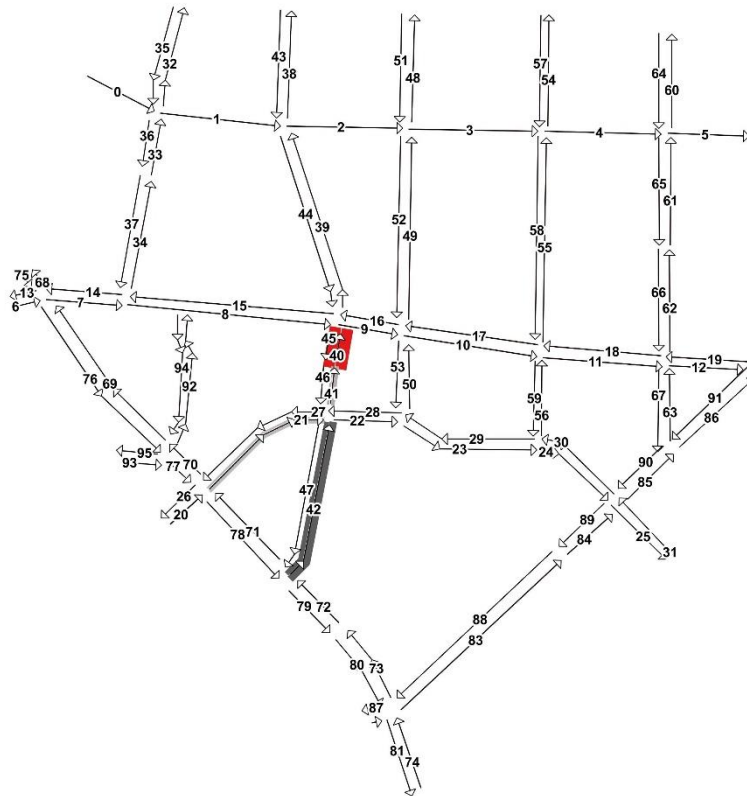
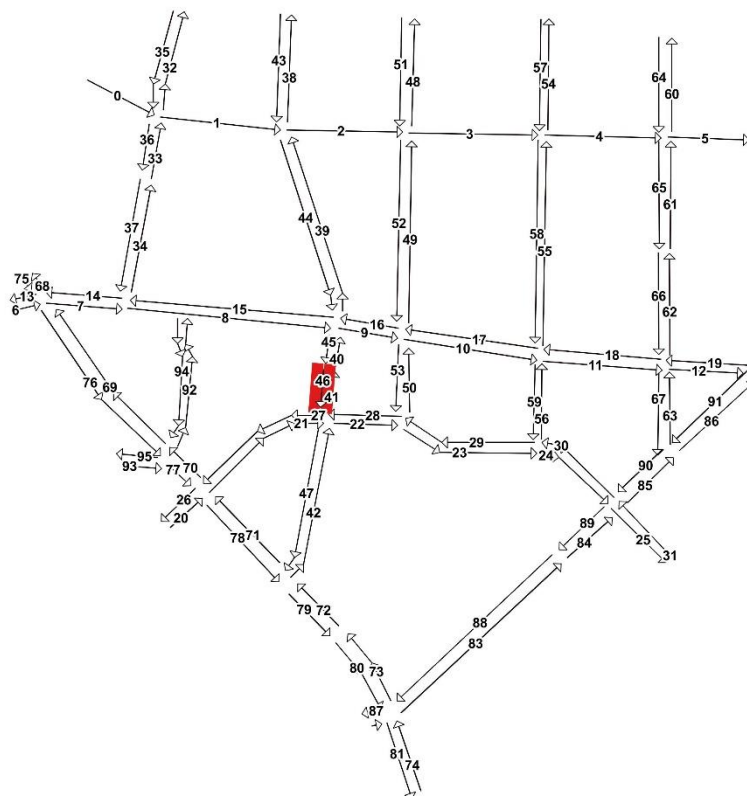Figure 4.17 Upstream Influence from The Congestion of Segment 40 (S2_avg)

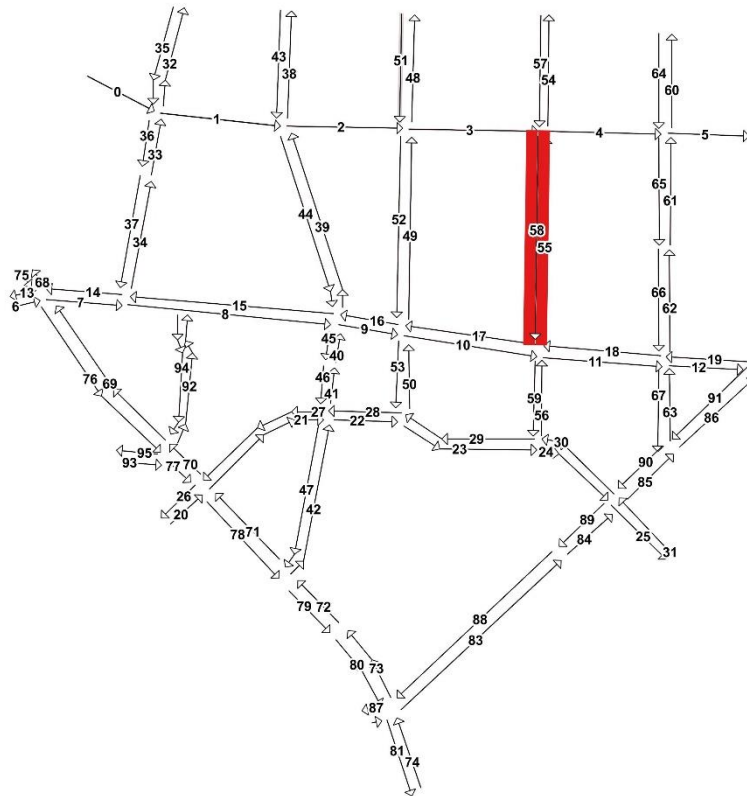Figure 4.18 Upstream Influence from The Congestion of Segment 46 (S2_avg)

52

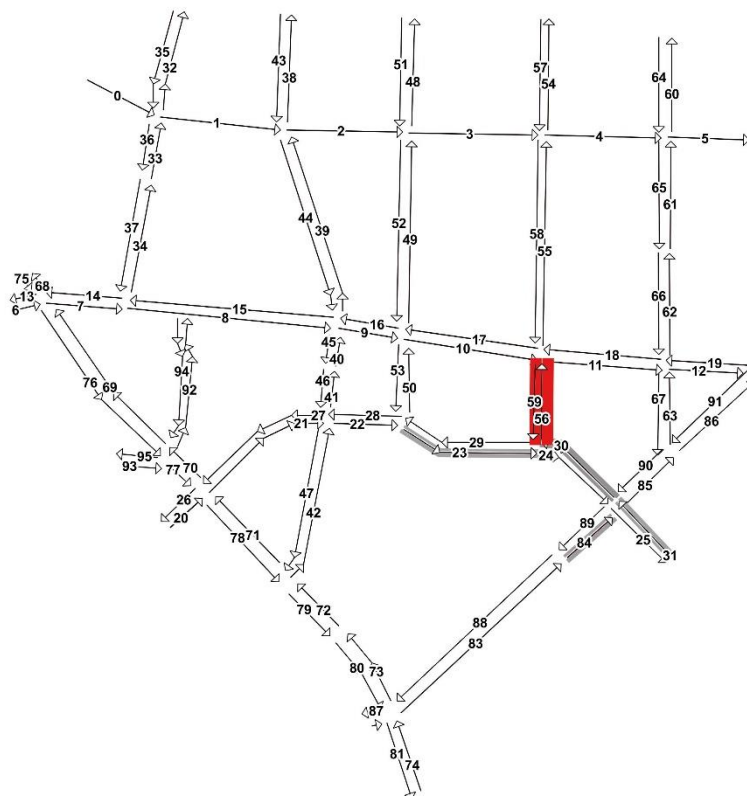Figure 4.19 Upstream Influence from The Congestion of Segment 58 (S2_avg)

Figure 4.20 Upstream Influence from The Congestion of Segment 56 (S2_avg)

53

4.3   Summary of Insights from Case Study

In this chapter, a case study with two scenarios during different time interval in the same urban road network is performed. An urban network is constructed, an adjusted KDE is developed and the results are visualized for the sake of further understanding of the hot spots of traffic congestion, relationship between road segments as well as the congestion propagation pattern. Based on the comprehensive analysis, we induce some research findings from the visualization results in both the overview and the segment-wise perspectives.

<u>Overview</u>

During the construction of bike lanes, layouts of road segments were changed. According to the report of Taipei City Traffic Engineering Office made about the evaluation of bike lane construction, travel speed has slightly decreased on the arterials with bike lane construction and recovered after the construction was completed. However, according to this research, the probability of the occurrence of the congestion has changed comparing to the data before the construction and are likely to be higher on the arterials with bike lane construction than elsewhere.

The analysis results from Scenario 1 show that for a day with special event, the size of the impacted area may increase, indicating that a single congestion incident is likely to spread wider. Based on threshold of the LOS C, usually most of the road segments performed quite well even during the bike lane construction. However, if we use the average speed criterion, which represents the daily traffic baseline, it shows that fluctuations of the travel speed and congestion incidents actually happen from time to time. Hence, a varying value of average travel speed may be a better standard for more
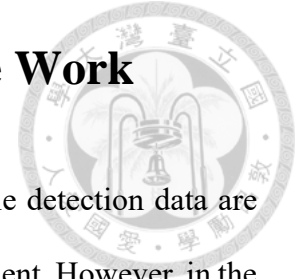
active traffic management.

Segment-wise

Road segments of the 1st order adjacency usually have higher density than road segments of the 2nd order adjacency, which is consistent with the common knowledge of traffic management that spatially closer locations have stronger connection to each other.

For the connections of the road segment of congestion source and its 1st order adjacent upstream road segments, we may conclude that generally the upstream which goes straight to the congested road segment is affected most by the source. The segment with a left turn comes second and the segment with a right turn receives the least influence. For the connections between road segment of the 1st order adjacency and road segments of the 2nd order adjacency, similar characteristics can be observed. Each road segment in a grid network can have at most three 1st order adjacent upstream road segments and nine 2nd order adjacent upstream road segments. However, not every road segment within the road network is orthogonally connected with each other. Additionally, not all of them have VDs installed. Hence, there may be some simplifications in this study. However, the proposed approach can be sufficient for the research objectives and flexible for extended applications.
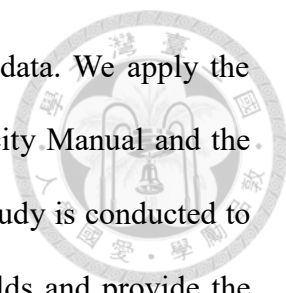
55

Chapter 5 Conclusions and Future Work

Due to the advanced sensor technology, high-resolution vehicle detection data are accessible and can provide abundant information for traffic management. However, in the existing literature, these data have not been fully explored and utilized. Hence, this research develops a framework by using an adjusted KDE approach to estimate the effects of congestion propagation in an urban roadway network, through data preprocessing, analysis to visualization. Based on the VD data in Taipei City, this research presents a VD data analysis framework composed of congestion and incident detection, KDE, visualization of congestion hot spots and propagation patterns. The long-term bike lane network construction since 2014 is used for the case study to investigate the propagation pattern during network layout changes. Based on the proposed approach, this study concludes the research insights related to the forming, propagation and dissipation of the traffic congestion in the following sections.

5.1 Conclusions

Based on the research background, literature review, construction of a KDE based spatial analysis framework and the case study in Chapter 4, the research insights of this study can be concluded as follows:

(1) This research utilizes the adjusted kernel density estimation approach to compute the effects of congestion on road segments. By constructing the network structure, we not only record the location and adjacency of neighboring road segments, but also identify how they are connected in terms of traffic flow dynamics. This non parametric approach allows us to better understand the spatial characteristics of traffic flow evolution over a network.
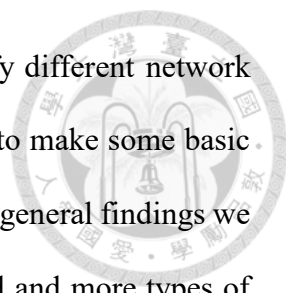
(2) This study displays a complete framework for analyzing VD data. We apply the criteria suggested from the latest 2011 version Highway Capacity Manual and the average travel speed calculated from the data itself. The case study is conducted to test the feasibility of applying them as the congestion thresholds and provide the visualized results, which can help identify the characteristics of congestion propagation patterns under different event and network layout changes.

(3) The relationship between neighboring road segments and the influence contributed by the congestion source segment are clarified. A pattern of congestion propagation can be found which is consistent with the general knowledge about traffic management. However, that some part of road network that is not a typical grid network has slightly different outcomes while most part of the network is typical and follows the general pattern. The proposed framework can still provide the visualization of propagation pattern for each road segment.

(4) Instead of plotting data on the time line to observe the fluctuation. The propagation of congestion may be visualized to some extent. However, this study contributes on several different perspectives. Our proposed methodology can not only visualize the propagation itself but also extract its characteristics. Furthermore, it has good expandability to compare with historical data and the ability to predict future traffic state with urban road network, which is valuable reference for traffic management.

57

5.2 Future Work

To further enhance the analysis of urban VD data and its applications for traffic management, there are several considerations and suggestions for the future work, which may expand the use of the data analysis framework and provide referential information for better quality decision-making. The relevant aspects are listed as follows:
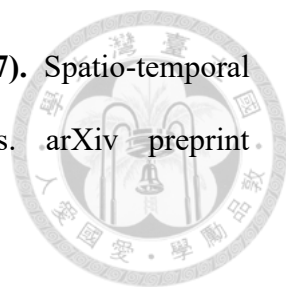
(1) To make the results more reliable, the malfunctioning rate and the amount of missing data need to be decreased. On the other hand, it may be addressed by either installing more VDs to fill the vacancy spot or developing proper data imputation approaches. The reliability of different data imputation approach need to be further tested as well.

(2) New data can be further included to form a larger data set. More generalized base line traffic conditions can be determined. Also, by arbitrarily choosing certain part of data set for more case studies, the congestion propagation pattern under different circumstances can be identified. The outcome can be provided as a network evaluation reference for transportation engineering and management agencies.

(3) For the adjusted network KDE approach proposed in this study, the spatial relationship of road segments and the conditional probability p_{is} are considered in the equation. However, in p_{is} the closeness between congestion incidents in terms of time dimension is not directly used. Hence, elements that can properly represent the time dimension can be further investigated.

(4) There are some difficulties in extracting road network information. For example, road networks may not always be typical grid network and the map information is not well organized or reliable. Problems for constructing small networks may be fixed manually. However, to implement this approach to a larger network, automatic network extracting technique need to be further developed.

58

(5) More studies can be conducted by focusing on how to simplify different network structures while extracting their commonality. We may be able to make some basic explanation about some phenomenon slightly different from the general findings we come up with. However, what kind of simplification is allowed and more types of road segment connection patterns still need further investigation.
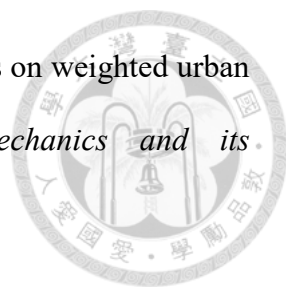
REFERENCE

[1] **Anbaroglu, B., Heydecker, B., & Cheng, T. (2014).** Spatio-temporal clustering for non-recurrent traffic congestion detection on urban road networks. *Transportation Research Part C: Emerging Technologies*, *48*, 47-65.

[2] **Chen, W., Guo, F., & Wang, F. Y. (2015).** A survey of traffic data visualization. *IEEE Transactions on Intelligent Transportation Systems*, *16*(6), 2970-2984.

[3] **Chen, Z., Liu, X. C., & Zhang, G. (2016).** Non-recurrent congestion analysis using data-driven spatiotemporal approach for information construction. *Transportation Research Part C: Emerging Technologies*, *71*, 19-31.

[4] **Coifman, B. (2002).** Estimating travel times and vehicle trajectories on freeways using dual loop detectors. *Transportation Research Part A: Policy and Practice*, *36*(4), 351-364.

[5] **Coifman, B. (2003).** Identifying the onset of congestion rapidly with existing traffic detectors. *Transportation Research Part A: Policy and Practice*, *37*(3), 277-291.

[6] **Daqing, L., Yinan, J., Rui, K., & Havlin, S. (2014).** Spatial correlation analysis of cascading failures: congestions and blackouts. *Scientific reports*, *4*, 5381.

[7] **Ji, Y., Luo, J., & Geroliminis, N. (2014).** Empirical observations of congestion propagation and dynamic partitioning with probe data for large-scale systems. *Transportation Research Record: Journal of the Transportation Research Board*, (2422), 1-11.

[8]   **Jiang, Y., Kang, R., Li, D., Guo, S., & Havlin, S. (2017).** Spatio-temporal propagation of traffic jams in urban traffic networks. arXiv preprint arXiv:1705.08269.

[9]   **Kerner, B. S., Demir, C., Herrtwich, R. G., Klenov, S. L., Rehborn, H., Aleksic, M., & Haug, A. (2005, September).** Traffic state detection with floating car data in road networks. In *Intelligent Transportation Systems, 2005. Proceedings. 2005 IEEE* (pp. 44-49). IEEE.

[10]   **Kurihara, S., Tamaki, H., Numao, M., Yano, J., Kagawa, K., & Morita, T. (2009, May).** Traffic congestion forecasting based on pheromone communication model for intelligent transport systems. In *Evolutionary Computation, 2009. CEC'09. IEEE Congress on* (pp. 2879-2884). IEEE.

[11]   **Li, X., She, Y., Luo, D., & Yu, Z. (2013).** A traffic state detection tool for freeway video surveillance system. *Procedia-Social and Behavioral Sciences*, *96*, 2453-2461.

[12]   **Long, J., Gao, Z., Ren, H., & Lian, A. (2008).** Urban traffic congestion propagation and bottleneck identification. *Science in China Series F: Information Sciences*, *51*(7), 948.

[13]   **Meng, L. M., Han, L. S., Peng, H., Zhang, B., & Du, K. L. (2014, August).** A machine learning approach to urban traffic state detection. In *Intelligent Control and Information Processing (ICICIP), 2014 Fifth International Conference on* (pp. 163-168). IEEE.

[14] **Mirge, V., Verma, K., & Gupta, S. (2017).** Dense traffic flow patterns mining in bi-directional road networks using density based trajectory clustering. *Advances in Data Analysis and Classification*, *11*(3), 547-561.

[15] **Nagatani, T. (2002).** The physics of traffic jams. *Reports on progress in physics*, *65*(9), 1331.

[16] **Ni, D., & Wang, H. (2008).** Trajectory reconstruction for travel time estimation. Journal of Intelligent Transportation Systems, 12(3), 113-125.

[17] **Parzen, E. (1962).** On estimation of a probability density function and mode. *The annals of mathematical statistics*, *33*(3), 1065-1076.

[18] **Rosenblatt, M. (1956).** Remarks on some nonparametric estimates of a density function. *The Annals of Mathematical Statistics*, 832-837.

[19] **Sun, Z., & Ban, X. J. (2013).** Vehicle trajectory reconstruction for signalized intersections using mobile traffic sensors. *Transportation Research Part C: Emerging Technologies*, *36*, 268-283.

[20] **Treiber, M., & Helbing, D. (2002).** Reconstructing the spatio-temporal traffic dynamics from stationary detector data. Cooperative Transportation Dynamics, 1(3), 3-1.

[21] **Wang, Z., Lu, M., Yuan, X., Zhang, J., & Van De Wetering, H. (2013).** Visual traffic jam analysis based on trajectory data. *IEEE Transactions on Visualization and Computer Graphics*, *19*(12), 2159-2168.

[22] **Wu, J. J., Sun, H. J., & Gao, Z. Y. (2007).** Cascading failures on weighted urban traffic equilibrium networks. *Physica A: Statistical Mechanics and its Applications*, *386*(1), 407-413.

[23] **Wu, Z. X., Peng, G., Wang, W. X., Chan, S., & Wong, E. W. M. (2008).** Cascading failure spreading on weighted heterogeneous networks. *Journal of Statistical Mechanics: Theory and Experiment*, *2008*(05), P05013.

[24] **Xie, Z., & Yan, J. (2008)**. Kernel density estimation of traffic accidents in a network space. *Computers, environment and urban systems*, *32*(5), 396-406.

[25] **Zhu, W., & Barth, M. (2006, September).** Vehicle trajectory-based road type and congestion recognition using wavelet analysis. In *Intelligent Transportation Systems Conference, 2006. ITSC'06. IEEE* (pp. 879-884). IEEE.

[26] 林豐博、曾平毅、林國顯、蘇振維、張瓊文、鄭嘉盈、呂怡青、劉國慶、陳昭堯、王怡方。**(2011)**。"2011 年臺灣公路容量手冊",交通部運輸研究所。

[27] 胡英浩。**(2012)**。"使用 GPS 軌跡資料推估遊客空間分布－以野柳地質公園為例",碩士論文,國立台灣大學地理環境資源研究所。

[28] 張正鼎。**(2012)**。"整合資料探勘與核密度估計技術於人體多重疾病共同生理指標之評估",博士論文,元智大學工業工程管理研究所。

[29] 葉志宏。**(2016)**。"臺北市政府交通局三橫三縱自行車路網施工影響說明",台北市交通工程管制處。

[30] 余孟冠。(2009)。"關於核密度函數估計之研究"，碩士論文，國立清華大學數學研究所。